Japanese version of the PHQ-9 also has excellent validity in primary care and in psychiatric settings [23,24]. A major depressive episode is diagnosed in two ways using the PHQ-9: it is diagnosed by a diagnostic algorithm and a summary score [19]. In this study, we adopted the diagnostic algorithm of the PHQ-9 for screening major and other types of depressive episodes because this algorithm is based on DSM-IV criteria. It is thus suitable for identifying other types of depressive episodes with similar criteria (2 to 4 characteristics) [19]. The diagnostic algorithmic threshold for diagnosing a major depressive episode was considered fulfilled if the answer to question #1a or question #1b and five or more of questions #1a–#1i was at least "more than half the days" (question #1i was counted if present at all). The diagnostic algorithmic threshold for diagnosing other depressive episode was regarded as fulfilled if the answer to question #1a or question #1b and two, three or four of questions #1a–#1i was at least "more than half the days" (question #1i was counted if present at all).

After reviewing the data, when an individual responded that he or she had, "Thoughts that you would be better off dead or of hurting yourself in some way" at least "several days" out of the week, subjects were considered to have "ideas of suicide or self-harm".

2.2.2. TCI

The TCI is a self-report method of personality testing based on a theory proposed by Cloninger [13]. In this study, we used the 125-item Japanese version of the TCI with a 4-point scale. Kijima et al. showed that a 4-point scale was superior to a dichotomous scale in terms of internal consistency, as expressed by Cronbach's α coefficient [25]. This Japanese version of the TCI is a valid and reliable measure of temperament and character for the young adult population [26]. *Character profiles* were created according to Cloninger's methods [27]. We then compared the prevalence of depressive episodes (major and other depressive episodes) and the prevalence of ideas of suicide or self-harm for at least "several days," as defined by the PHQ-9. To form the *character profiles*, the sample was divided into subjects above and below the median for each of the three character traits (i.e., SD, C, and ST) after excluding the 33 participants who were in the middle third of the distribution for all three traits. Then, the participants were grouped according to their character scores to define the eight possible character configurations shown in Table 1. The character profiles are listed in the order that was previously observed to be associated with less happiness and character integration [27]. The variables "s", "c", and "t" denote low SD scores, low C scores, and low ST scores, respectively. The variables "S", "C", and "T" denote high SD scores, high C scores, and high ST scores. Individuals who have sct *character profiles* are described as "melancholic" because they are selfish, immature, and emotionally reactive [15]. Individuals who have scT *character profiles* are designated as "disorganized" because they tend to be illogical, suspicious, and immature [15]. The countertype to the melancholic personality is the creative character (SCT). They are inventive, thoughtful, mature, and frequently feel the positive emotions of joy, love, and hope [15]. The organized character SCt is described as logical, trusting, and mature [15].

2.3. Statistical analyses

Descriptive statistics were given for demographic data and were subjected to chi-square tests and an analysis of variance (ANOVA). For an analysis of TCI scores, a two-way ANOVA was used. Diagnoses and gender were used as two categorical factors for the analyses because gender differences have been reported for the TCI [11,13]. Tukey's HSD test was applied as post-hoc analysis. We then analyzed the association between *character profiles* and depressive episodes or, ideas of suicide or self-harm. To confirm the order of character dimension, a logistic regression analysis was performed. Thereafter, the Cochran-Armitage trend test was performed to analyze the association between character maturity and the prevalence of depressive episodes or ideas of suicide or self-harm. Bonferroni corrections were made, and the differences were

Table 1
Demographic data.

	NC	Other	Major	Statistics	*P*
	N = 1283	N = 97	N = 41		
Gender[a]					
Female	377	36	15	$\chi^2 = 3.398$	0.183
Male	906	61	26		
Age, mean (S.D.)[b]					
Female	18.5 (1.2)	18.4 (0.7)	18.7 (0.9)	$F = 1.008$	0.366
Male	18.6 (1.6)	18.4 (0.6)	19.0 (1.9)	$F = 0.792$	0.453
PHQ-9 total score, mean (S.D.)[b]					
Female	3.2 (2.5)	11.4 (1.4)	17.7 (2.6)	$F = 388.3$	<0.000*
Male	3.1 (2.6)	11.4 (1.4)	18.6 (3.2)	$F = 673.3$	<0.000*

[a] Chi-square test.
[b] ANOVA; NC, non-depressive controls; Other, Other depressive episode; Major, Major depressive episode.
* Statistically significant.

considered significant at $P < 0.001$. SPSS software, version17.0 (SPSS Inc., Japan) and JMP pro10.0 (SAS Institute Inc., Japan) were used for our analysis.

3. Results

3.1. Demographic data

Demographic data were shown in Table 1. The ratio of male to female individuals was not significantly different between groups ($\chi^2 = 3.398$, $P = 0.138$). The ANOVA showed no significant difference in mean age between female groups ($F = 1.008$, $P = 0.366$) and male groups ($F = 0.792$, $P = 0.453$). Meanwhile, as expected, the ANOVA showed significant differences in PHQ-9 total scores between female groups ($F = 388.3$, $P < 0.001$) and male groups ($F = 673.3$, $P < 0.001$).

3.2. TCI scores

Mean TCI scores are shown in Table 2. Concerning interaction effects between gender and diagnosis, we performed a two-way ANOVA test (diagnosis × gender) (Table 3). The results of ANOVA revealed significant effects of diagnosis on HA scores ($F[2,1415] = 20.389$, $P < 0.001$), RD scores ($F[2,1415] = 10.051$, $P < 0.001$), SD scores ($F[2,1415] = 55.108$, $P < 0.001$), and C scores ($F[2,1415] = 16.292$, $P < 0.001$). Gender was also shown to have an effect on RD scores ($F[1,1415] = 14.089$, $P < 0.001$). No interaction effect, however, was found between gender and diagnosis when analyzing TCI scores (Table 3). We then performed a post-hoc analysis using the HSD test. No significant difference in TCI scores was found between major depressive episodes and other depressive episode groups. The major depressive episode group had significantly higher HA scores ($P < 0.001$), lower RD scores ($P < 0.001$), lower SD scores ($P < 0.001$), and lower C scores ($P < 0.001$) than did non-depressive controls. The other depressive episode group had significantly higher HA scores ($P < 0.001$) and lower SD scores ($P < 0.001$) than did the non-depressive controls.

3.3. Character profiles of major and other depressive episodes and ideas of suicide or self-harm

A logistic regression analysis revealed that SD had the greatest contribution to major and other depressive episodes, followed by C (Table 4). ST did not contribute to major or other depressive episodes significantly. We compared the prevalence of major and other depressive episodes among four categories of possible combinations, which were sc (sct, scT), sC (sCt, sCT), Sc (Sct, ScT), and SC (SCt, SCT). The major or other depressive episodes were observed frequently (16.1%) in individuals who were depressive (sct) or disorganized (scT). Alternately, these episodes were rarely observed (2.2%) in individuals who were creative (SCT) or organized (SCt) (Table 5). The Cochran-Armitage trend test revealed that the prevalence of depressive episodes increased as SD and C scores lowered, i.e., *character profiles* became immature ($\chi^2_{trend} = 57.2$, $P < 0.0001$). The same tendency was also observed for ideas of suicide or self-harm ($\chi^2_{trend} = 49.3$, $P < 0.0001$) (Table 6).

4. Discussion

In this study, we confirmed that young adults with major and other depressive episodes had higher HA scores and lower SD scores than did non-depressive controls. A significant difference in personality traits between individuals with major and other depressive episodes was not observed. As low SD and low C scores increased in number, the prevalence of major and other depressive episodes, as well as ideas of suicide or self-harm, tended to increase. These results suggest that *character profiles* with high SD and high C scores are protective factors against depressive episodes and ideas of suicide or self-harm among young adults.

Table 2
Comparison of TCI scores among non-depressive controls (NC), other depressive episode group (Other) and major depressive episode group (Major).

	NC (N = 1283)		Other (N = 97)		Major (N = 41)	
	Female	Male	Female	Male	Female	Male
	(N = 377)	(N = 906)	(N = 36)	(N = 61)	(N = 15)	(N = 26)
	Mean (S.D.)	Mean (S.D.)	Mean (S.D.)	Mean (S.D.)	Mean (S.D.)	Mean (S.D.)
Temperament						
NS	49.5 (6.7)	49.8 (6.4)	52.3 (8.5)	49.9 (7.0)	50.1 (5.7)	51.7 (6.9)
HA	55.3 (9.4)	55.4 (9.0)	57.7 (11.1)	61.1 (9.9)	63.7 (5.2)	62.5 (7.7)
RD	45.6 (5.6)	43.2 (5.5)	45.5 (5.9)	41.5 (6.2)	41.3 (6.8)	39.4 (8.6)
P	10.8 (2.7)	10.3 (2.8)	9.9 (3.2)	10.2 (2.9)	11.1 (3.9)	9.7 (4.0)
Character						
SD	89.2 (9.0)	86.7 (9.7)	79.5 (11.2)	78.0 (8.8)	77.8 (10.0)	78.3 (12.3)
C	75.4 (7.7)	72.9 (7.8)	74.1 (7.6)	69.4 (8.5)	68.1 (10.0)	66.9 (11.8)
ST	15.1 (6.8)	14.2 (6.9)	17.9 (6.9)	13.2 (8.1)	16.2 (6.8)	13.1 (8.1)

NS; Novelty Seeking, HA; Harm Avoidance, RD; Reward Dependence, P; Persistence, SD; Self-Directedness, C; Cooperativeness, ST; Self-Transcendence.

Table 3
Comparison of TCI scores using a two-way ANOVA.

	Source of variations	F statistic	P	Tukey HSD test		
				Major vs. Other	Major vs. NC	Other vs. NC
NS	Gender	0.033	0.855			
	Diagnosis	2.532	0.080	-	-	-
	Gender × diagnosis	1.869	0.155			
HA	Gender	0.400	0.527			
	Diagnosis	20.389	<0.001*	0.168	<0.001↑*	<0.001↑*
	Gender × diagnosis	1.566	0.209			
RD	Gender	14.089	<0.001*	(Female > Male)		
	Diagnosis	10.051	<0.001*	0.015	<0.001↓*	0.307
	Gender × diagnosis	0.906	0.404			
P	Gender	2.044	0.153			
	Diagnosis	1.105	0.332	-	-	-
	Gender × diagnosis	1.236	0.291			
SD	Gender	0.859	0.354			
	Diagnosis	55.108	<0.001*	0.966	<0.001↓*	<0.001↓*
	Gender × diagnosis	0.517	0.596			
C	Gender	7.349	0.007			
	Diagnosis	16.292	<0.001*	0.029	<0.001↓*	0.006
	Gender × diagnosis	0.940	0.391			
ST	Gender	10.039	0.002			
	Diagnosis	0.644	0.526	-	-	-
	Gender × diagnosis	3.429	0.033			

Major; Major depressive episode group, Other; Other depressive episode group, NC; Non-depressive controls, NS; Novelty Seeking, HA; Harm Avoidance, RD; Reward Dependence, P; Persistence, SD; Self-Directedness, C; Cooperativeness, ST; Self-Transcendence.
↑, higher in major or other depressive groups than in NC.
↓, lower in major or other depressive groups than in NC.
* Statistically significant.

In this study, high HA scores were observed in both the major depressive episode group and other depressive episode group. Harm avoidance is the temperament dimension that corresponds to the inhibition of behavior [28]. Thus, individuals who had high harm avoidance scores tended to have anticipatory worry, fear of uncertainty, shyness, and rapid fatigability [13]. These features of HA may predispose the subjects to depression [28]. High HA scores in major depressive disorder were reported repeatedly in clinical settings [6,29,30]. That being said, temperaments of individuals with minor depressive episodes, which correspond to other depressive episodes defined by the PHQ-9, have not been studied. In our study, HA scores in the other depressive episode group were as high as those in the major depressive episode group. Previous findings showed that high HA scores reflect a depressive trait [14,31–33] and that minor depression is a predictor of major depressive disorder [8]. Consistent with these results, the results of this study indicate that high HA scores are a common temperament trait of major and other depressive episodes.

Table 4
Logistic regression analysis to confirm the effect size of character dimensions.

	SE	Wald	OR	P	95% C.I.
SD	0.011	53.681	1.086	0.000	1.062–1.110
C	0.013	9.264	1.041	0.002	1.014–1.069
ST	0.014	2.978	0.976	0.084	0.949–1.003

SE, Standard error, OR, Odds ratio, C.I., Confidence interval.

Low RD scores were observed only in the major depressive episode group. Previous studies involving young adults reported a correlation between depressive symptoms and low RD scores [2–4]. Kampman and Poutanen suggested that low RD scores in depression may be state-dependent because low RD scores were raised by treatment during clinical trials [6]. Therefore, low RD scores may be a sign of severe and untreated depressive symptoms. In the future, we will conduct a longitudinal study to follow-up the same group of university students and to evaluate whether a low RD score is a result of state effects of depression or a trait, which might lead to depression.

Table 5
Major or other depressive episode and character profiles.

Character profiles			Non-depressive controls	Major or other depressive episode	Total	%
sc	sct	Depressive	396	76	472	16.1%
	scT	Disorganized				
sC	sCt	Dependent	210	37	247	15.0%
	sCT	Moody				
Sc	Sct	Autocratic	252	14	266	5.3%
	ScT	Fanatical				
SC	SCt	Organized	394	9	403	2.2%
	SCT	Creative				

Cochran-Armitage trend test; $\chi^2_{trend} = 57.2$, $P < 0.0001$, $\chi^2_{linearity} = 3.83$, $P = 0.28$.

Table 6
Ideas of suicide or self-harm and character profiles.

Character profiles			No. of subjects without ideas of suicide or self-harm	No. of subjects with ideas of suicide or self-harm	Total	% of ideas of suicide or self-harm
sc	sct	Depressive	406	66	472	14.0%
	scT	Disorganized				
sC	sCt	Dependent	221	26	247	10.5%
	sCT	Moody				
Sc	Sct	Autocratic	253	13	266	4.9%
	ScT	Fanatical				
SC	SCt	Organized	396	7	403	1.7%
	SCT	Creative				

Cochran-Armitage trend test; $\chi^2_{trend} = 49.3$, $P < 0.0001$, $\chi^2_{linearity} = 0.41$, $P = 0.94$.

In this study, Japanese young adults with major or other depressive episodes showed lower SD and C scores. When the *character profiles* of participants had low SD and low C, the prevalence of depressive episodes and ideas of suicide or self-harm was markedly increased. This result suggests that *character profiles* with low SD and/or low C would have a strong impact on the prevalence of depressive episodes and ideas of suicide or self-harm among young adult populations. In previous studies, both low SD scores and low C scores were shown during major depression in clinical settings [14,15]. Conversely, previous studies have also demonstrated that only SD scores in the character dimension were negatively associated with depressive symptoms [5,14,34]. The character dimension of SD measures self-determination and the ability of an individual to control a situation in accordance with their individually chosen goals and values [13]. The character dimension of C measures an individual's social tolerance, empathy, helpfulness, and compassion [13]. In our study, the combination of high SD and C seems to lower the risk of depressive episodes and ideas of suicide or self-harm. Moreover, a recent study on well-being, which is a broader concept of mental health, reported that character has a strong impact on all aspects of health, including social, emotional, and physical well-being [27]. The evaluation of *character profiles* using the TCI is useful for a broad assessment of mental health among young adult populations. This study suggests that a relationship exists between depression and *character profiles*.

Cross-sectional design proved to be a limitation of this study. In the future, longitudinal studies will be needed to analyze the risks and protective factors for major depressive disorders and ideas of suicide or self-harm. The association between *character profiles* and oncoming depression or suicide needs to be studied further. Another limitation of this study was that "other depressive episode" derived from the PHQ-9 includes not only minor depressive episode but also dysthymia and other depressive disorders not otherwise specified in DSM-IV. Although time-consuming, structured clinical interviews are necessary to overcome this limitation; therefore, it is difficult to apply these interviews to a large-scale screening test, such as in this study. Finally, in this study, we evaluated ideas of suicide or self-harm by the item of PHQ-9. However, the relationship between suicide and self-injurious behaviors is reportedly complex in a college population. More than half of the students who had engaged in self-injurious behaviors reported never having considered or attempted suicide [35]. Accordingly, ideas of self-harm are not always related to suicidal ideas. That we could not distinguish between ideas of suicide and those of self-harm is also one limitation in this study.

In conclusion, high HA scores, low RD scores, low SD scores and low C scores were prevalent in young adults who had major depressive episodes. High HA scores and low SD scores were also common in our major and other depressive episode groups. *Character profiles* have a strong impact on the prevalence of major depressive episodes, depressive episodes and ideas of suicide or self-harm.

Acknowledgment

This study was partly supported by the program, "Integrated research on neuropsychiatric disorders" carried out under the Strategic Research Program for Brain Sciences by the Ministry of Education, Culture, Sports, Science, and Technology of Japan, a Research Grant 24–2 for Nervous and Mental Disorders from the Ministry of Health, Labor and Welfare, and a grant from the Interdisciplinary Project for Psychosomatological Research in Hokkaido University.

References

[1] Kessler RC, Borges G, Walters EE. Prevalence of and risk factors for lifetime suicide attempts in the National Comorbidity Survey. Arch Gen Psychiatry 1999;56:617-26.
[2] Matsudaira T, Kitamura T. Personality traits as risk factors of depression and anxiety among Japanese students. J Clin Psychology 2006;62:97-109.
[3] Naito M, Kijima N, Kitamura T. Temperament and Character Inventory (TCI) as predictors of depression among Japanese college students. J Clin Psychology 2000;56:1579-85.
[4] Peirson A, Heuchert J. The relationship between personality and mood: comparison of the BDI and the TCI. Pers Individ Dif 2001;30:391-9.
[5] Tanaka E, Kijima N, Kitamura T. Correlations between the Temperament and Character Inventory and the Self-rating Depression Scale among Japanese Students. Psychol Rep 1997;80:251-4.
[6] Kampman O, Poutanen O. Can onset and recovery in depression be predicted by temperament? A systematic review and meta-analysis. J Affect Disord 2011;135:20-7.
[7] Cuijpers P, Smit F. Subthreshold depression as a risk indicator for major depressive disorder: a systematic review of prospective studies. Acta Psychiatr Scand 2004;109:325-31.
[8] Fogel J, Eaton WW, Ford DE. Minor depression as a predictor of the first onset of major depressive disorder over a 15-year follow-up. Acta Psychiatr Scand 2006;113:36-43.
[9] Johnson JG, Cohen P, Kasen S. Minor depression during adolescence and mental health outcomes during adulthood. Br J Psychiatry 2009;195:264-5.

[10] Svrakic DM, Whitehead C, Przybeck TR, Cloninger CR. Differential diagnosis of personality disorders by the seven-factor model of temperament and character. Arch Gen Psychiatry 1993;50:991-9.
[11] Bayon C, Hill K, Svrakic DM, Przybeck TR, Cloninger CR. Dimensional assessment of personality in an out-patient sample: relations of the systems of Millon and Cloninger. J Psychiatr Res 1996;30:341-52.
[12] Cloninger C. Feeling good: the science of well being. New York: Oxford University Press; 2004.
[13] Cloninger CR, Svrakic DM, Przybeck TR. A psychobiological model of temperament and character. Arch Gen Psychiatry 1993;50:975-90.
[14] Cloninger CR, Svrakic DM, Przybeck TR. Can personality assessment predict future depression? A twelve-month follow-up of 631 subjects. J Affect Disord 2006;92:35-44.
[15] Cloninger CR, Bayon C, Svrakic DM. Measurement of temperament and character in mood disorders: a model of fundamental states as personality types. J Affect Disord 1998;51:21-32.
[16] Conrad R, Walz F, Geiser F, Imbierowicz K, Liedtke R, Wegener I. Temperament and character personality profile in relation to suicidal ideation and suicide attempts in major depressed patients. Psychiatry Res 2009;170:212-7.
[17] Calati R, Giegling I, Rujescu D, Hartmann AM, Moller HJ, De Ronchi D, et al. Temperament and character of suicide attempters. J Psychiatr Res 2008;42:938-45.
[18] Mitsui N, Asakura S, Inoué T, Shimizu Y, Fujii Y, Kako Y, et al. Temperament and character profiles of Japanese university students with suicide completion. Compr Psychiatry 2013;54:556-61.
[19] Spitzer RL, Kroenke K, Williams JB. Validation and utility of a self-report version of PRIME-MD: the PHQ primary care study. JAMA 1999;282:1737-44.
[20] Gilbody S, Richards D, Brealey S, Hewitt C. Screening for depression in medical settings with the Patient Health Questionnaire (PHQ): a diagnostic meta-analysis. J Gen Intern Med 2007;22:1596-602.
[21] Furukawa TA. Assessment of mood: guides for clinicians. J Psychosom Res 2010;68:581-9.
[22] Wittkampf KA, Naeije L, Schene AH, Huyser J, van Weert HC. Diagnostic accuracy of the mood module of the Patient Health Questionnaire: a systematic review. Gen Hosp Psychiatry 2007;29:388-95.
[23] Muramatsu K, Miyaoka H, Kamijima K, Muramatsu Y, Yoshida M, Otsubo T, et al. The patient health questionnaire, Japanese version: validity according to the mini-international neuropsychiatric interview-plus. Psychol Rep 2007;101:952-60.
[24] Inoue T, Tanaka T, Nakagawa S, Nakato Y, Kameyama R, Boku S, et al. Utility and limitations of PHQ-9 in a clinic specializing in psychiatric care. BMC Psychiatry 2012;12:73.
[25] Kijima NSR, Takeuchi M, Yoshino A, Ono Y, Kato M, et al. Cloninger's seven-factor model of temperament and character and Japanese version of Temperament and Character Inventory (TCI). Arch Psychiatr Diag Clin Eval 1996;7:379-99.
[26] Takeuchi M, Miyaoka H, Tomoda A, Suzuki M, Lu X, Kitamura T. Validity and reliability of the Japanese version of the Temperament and Character Inventory: a study of university and college students. Compr Psychiatry 2011;52:109-17.
[27] Cloninger CR, Zohar AH. Personality and the perception of health and happiness. J Affect Disord 2011;128:24-32.
[28] Cloninger CR. Temperament and personality. Curr Opin Neurobiol 1994;4:266-73.
[29] Hur JW, Kim YK. Comparison of Clinical Features and Personality Dimensions between Patients with Major Depressive Disorder and Normal Control. Psychiatry investig 2009;6:150-5.
[30] Hansenne M, Reggers J, Pinto E, Kjiri K, Ajamier A, Ansseau M. Temperament and character inventory (TCI) and depression. J Psychiatr Res 1999;33:31-6.
[31] Elovainio M, Kivimaki M, Puttonen S, Heponiemi T, Pulkki L, Keltikangas-Jarvinen L. Temperament and depressive symptoms: a population-based longitudinal study on Cloninger's psychobiological temperament model. J Affect Disord 2004;83:227-32.
[32] Smith DJ, Duffy L, Stewart ME, Muir WJ, Blackwood DH. High harm avoidance and low self-directedness in euthymic young adults with recurrent, early-onset depression. J Affect Disord 2005;87: 83-9.
[33] Ekinci O, Albayrak Y, Ekinci AE. Temperament and character in euthymic major depressive disorder patients: the effect of previous suicide attempts and psychotic mood episodes. Psychiatry investig 2012;9:119-26.
[34] Farmer A, Mahmood A, Redman K, Harris T, Sadler S, McGuffin P. A sib-pair study of the Temperament and Character Inventory scales in major depression. Arch Gen Psychiatry 2003;60:490-6.
[35] Whitlock J, Eckenrode J, Silverman D. Self-injurious behaviors in a college population. Pediatrics 2006;117:1939-48.

Neuropharmacology 67 (2013) 326–330

Contents lists available at SciVerse ScienceDirect

Neuropharmacology

journal homepage: www.elsevier.com/locate/neuropharm

Activation of β-adrenoceptors in the bed nucleus of the stria terminalis induces food intake reduction and anxiety-like behaviors

Tomonori Naka [a], Soichiro Ide [a], Tomokazu Nakako [a], Mikie Hirata [a], Yuki Majima [a], Satoshi Deyama [a], Hiroshi Takeda [b], Mitsuhiro Yoshioka [c], Masabumi Minami [a,*]

[a] Department of Pharmacology, Graduate School of Pharmaceutical Sciences, Hokkaido University, Sapporo 060-0812, Japan
[b] Laboratory of Pathophysiology and Therapeutics, Graduate School of Pharmaceutical Sciences, Hokkaido University, Sapporo 060-0812, Japan
[c] Department of Neuropharmacology, Graduate School of Medicine, Hokkaido University, Sapporo 060-8638, Japan

ARTICLE INFO

Article history:
Received 20 February 2012
Received in revised form
23 November 2012
Accepted 24 November 2012

Keywords:
Anxiety
Food intake
Bed nucleus of the stria terminalis
Emotion
Noradrenaline

ABSTRACT

We previously demonstrated the critical role of noradrenergic transmission within the ventral part of the bed nucleus of the stria terminalis (vBNST) in pain-induced aversion. We showed that activation of β-adrenoceptors in this brain region by intra-vBNST injection of isoproterenol, a β-adrenoceptor agonist, produced aversive responses. In the present study, we examined the effects of a β-adrenoceptor agonist injected into the vBNST on food intake and anxiety-like behaviors in male Sprague-Dawley rats. Bilateral intra-vBNST injection of isoproterenol (3 and 10 nmol/side) caused a dose-dependent decrease in food intake; this suppressive effect was reversed by co-administration of timolol, a β-adrenoceptor antagonist. Dose-dependent (10 and 30 nmol/side) induction of anxiety-like behaviors by isoproterenol was observed in the elevated plus maze (EPM) test, which was also reversed by co-administration of timolol. Off-site control injections of isoproterenol into the lateral ventricle did not show any significant effect in the food consumption and EPM tests. These results suggest that the vBNST is one of the neuroanatomical substrates which may be involved in the close relationship between negative affective states and reduction of food intake, and that noradrenergic transmission within this brain region plays a critical role in inducing anxiety-like behaviors and reduced food intake.

1. Introduction

A close relationship between anorexia and anxiety has been suggested. Pollice et al. (1997) showed a significant relationship between anorexia and anxiety disorders. Godart et al. (2000) reported that 83% of patients with anorexia nervosa had at least one lifetime diagnosis of an anxiety disorder. These findings suggest that common neuroanatomical substrates and neurotransmission mechanisms may mediate reduction of food intake and anxiety. The bed nucleus of the stria terminalis (BNST) is a limbic structure involved in stress responses and the regulation of negative affective states, such as anxiety and fear (Walker et al., 2003). The BNST has also been implicated in the regulation of food intake (Ciccocioppo et al., 2003). Thus, this brain region may be involved in the close relationship between negative affective states and reduction of food intake.

The BNST, especially its ventral part (vBNST), is densely innervated by noradrenergic fibers arising mainly from the nuclei of the solitary tract (including the A2 cell group) and caudal ventrolateral medulla (including the A1 cell group) (Woulfe et al., 1990; Forray et al., 2000). Noradrenergic transmission within the vBNST is important for mediating negative affective states. Specifically, suppression of noradrenergic neurotransmission in the vBNST attenuates fox odor-induced freezing behaviors (Fendt et al., 2005) and morphine withdrawal-induced conditioned place aversion (CPA) (Delfs et al., 2000) in rats. We previously demonstrated the crucial role of enhanced noradrenergic transmission via β-adrenoceptors within the vBNST in pain-induced CPA in rats (Deyama et al., 2008, 2009). We showed that activation of β-adrenoceptors in this brain region by intra-vBNST injection of isoproterenol, a β-adrenoceptor agonist, produced aversive responses. In the present study, we examined the effects of β-adrenoceptor activation within the vBNST on food intake and anxiety-like behaviors in rats.

2. Materials and methods

2.1. Animals

Male Sprague-Dawley rats (190–300 g; Japan SLC, Hamamatsu, Japan) were used. Three to four rats were housed per cage. After implantation of guide

* Corresponding author. Tel.: +81 11 706 3246; fax: +81 11 706 4987.
E-mail address: mminami@pharm.hokudai.ac.jp (M. Minami).

0028-3908/$ – see front matter © 2012 Elsevier Ltd. All rights reserved.
http://dx.doi.org/10.1016/j.neuropharm.2012.11.021

cannulae, the rats were individually housed in cages. All rats were housed under standard conditions (temperature 23 ± 1 °C, 12 h light/dark cycle, water available *ad libitum*). Food was also available *ad libitum*, except during the food-deprivation period. Naïve animals were used for each experiment. All experiments were approved by the institutional animal care and use committee of Hokkaido University.

2.2. Drugs

Isoproterenol (β-adrenoceptor agonist) and timolol (β-adrenoceptor antagonist) were purchased from Sigma (St Louis, MO). These drugs were dissolved in phosphate-buffered saline.

2.3. Microinjection

Under sodium pentobarbital anesthesia (50 mg/kg, i.p.), each rat was bilaterally implanted with 25-gauge stainless steel guide cannulae 1.5 mm above the vBNST (−0.3 mm rostral, 1.6 mm lateral, 6.0 mm ventral to the bregma) or lateral ventricle (−0.8 mm rostral, 1.4 mm lateral, 2.7 mm ventral to the bregma) according to the brain atlas (Paxinos and Watson, 1998). The rats were allowed to recover for at least 5 days and were handled for 1–2 min each day for habituation. Microinjection was performed using 33-gauge stainless steel injection cannulae inserted bilaterally into the guide cannulae. The injection cannulae protruded 1.5 mm from the tip of the guide cannulae to reach the vBNST or lateral ventricle. The injection cannulae were attached to a microinjection pump (CMA, Stockholm, Sweden) via PE 8 tubing. Drugs or vehicle were bilaterally administered into the vBNST in a volume of 0.5 μl/side at a rate of 0.5 μl/min, and the injection cannulae were left in place for 1 min after the injection to prevent backflow.

2.4. Food consumption test

Food intake was measured for 24 h, and then the animals were deprived of food for 20 h. Five min after the injection of isoproterenol (3 or 10 nmol/side), isoproterenol (10 nmol/side) plus timolol (10 nmol/side), or vehicle into the bilateral vBNST or lateral ventricle, food was given to the food-deprived rats, and food intake during 30 min was measured. The data are expressed as the food intake adjusted by the body weight of each rat (g/kg).

2.5. Elevated plus maze test

The apparatus used for the elevated plus maze (EPM) test was a cross-shaped maze composed of two open arms (10 × 50 cm) and two closed arms (10 × 50 cm with walls 45 cm in height) connected by a central platform (10 × 10 cm). The apparatus was elevated 50 cm from the floor, and illuminated by dim light (~20 lux at the central platform). Five minutes after microinjection, each rat was placed on the central platform facing an open arm. Then the animals were allowed to freely explore the apparatus for 10 min. The movement of each animal was recorded by video camera and analyzed using the software package LimeLight2 (Actimetrics, Wilmette, IL) to determine the time spent in open arms and the number of entries to closed arms.

2.6. Rotarod test

The effect of intra-vBNST isoproterenol injection on coordinated motor function was assessed using an accelerating rotarod apparatus (Med-Associates, St. Albans, VT). The rotarod accelerated constantly from 4 to 40 rpm over 5 min. Each rat was trained once a day for 2 days on the apparatus before the test day. On the test day, isoproterenol (30 nmol/side) or vehicle was injected into the bilateral vBNST. Five minutes after microinjection, each rat was placed on the rod and time spent on the rod was measured.

2.7. Histology

After behavioral experiments, histological analyses were performed to examine the placements of injection cannulae. Briefly, rats were decapitated and the brain was rapidly removed and frozen in powdered dry ice. Coronal sections (50 μm) were prepared on a cryostat, and stained with thionin. These sections were examined by light microscopy (40×). Data from rats with correct placements of the bilateral injection cannulae (Fig. 1) were used for statistical analyses.

2.8. Statistical analyses

The data are expressed as means ± SEM. Food intake and the time spent in the open arms and the number of closed arm entries in the EPM test were analyzed using one- or two-way analysis of variance (ANOVA) followed by the Newman–Keuls *post hoc* test, or using Student's *t*-test. Time spent on the rod in the rotarod test was analyzed using Student's *t*-test. Differences with $P < 0.05$ were considered significant.

3. Results

3.1. Effect of intra-vBNST injection of isoproterenol on food intake

Before food deprivation, no significant differences were observed in food intake for 24 h among the three groups (3, 10 nmol/side isoproterenol and vehicle; 95.1 ± 3.5, 97.0 ± 2.9 and 95.5 ± 3.1 g/kg/24 h, respectively). After food deprivation for 20 h, isoproterenol (3 or 10 nmol/side) or vehicle was injected into the bilateral vBNST, and then food intake was measured for 30 min. As shown in Fig. 2A, intra-vBNST injection of isoproterenol reduced food intake in a dose-dependent manner. One-way ANOVA showed a significant difference among groups ($F_{2, 16} = 12.86$, $P < 0.001$). *Post hoc* comparisons by Newman–Keuls test indicated that isoproterenol at a dose of 10 nmol/side significantly decreased food intake (7.61 ± 0.67 g/kg/30 min, $P < 0.001$) compared to the vehicle-injected group (16.4 ± 1.6 g/kg/30 min).

Off-site control experiments were carried out by injecting isoproterenol into the lateral ventricle at a dose of 10 nmol/side. Before food deprivation, no significant differences were observed in food intake for 24 h between the two groups (10 nmol/side isoproterenol and vehicle; 100.8 ± 2.8 and 101.0 ± 1.3 g/kg/24 h, respectively). After food deprivation for 20 h, isoproterenol (10 nmol/side) or vehicle was injected intracerebroventricularly, and then food intake was measured for 30 min. As shown in Fig. 2B, there was no significant difference in food intake between the isoproterenol- and vehicle-injected groups (16.0 ± 3.0 and 14.4 ± 1.0 g/kg/30 min, respectively; $P > 0.05$, Student's *t*-test).

3.2. Effect of co-administration of timolol on the reduction of food intake by isoproterenol

Next, we examined the effect of co-administration of timolol, a β-adrenoceptor antagonist, on the reduction of food intake induced by intra-vBNST injection of isoproterenol (Fig. 3). Two-way ANOVA indicated a significant main effect of isoproterenol ($F_{1, 26} = 13.1$, $P < 0.01$) and a significant interaction between the effects of isoproterenol and timolol ($F_{1, 26} = 5.05$; $P < 0.05$). Reduction of food intake induced by isoproterenol (7.31 ± 1.16 g/kg/30 min) was significantly reversed by co-administration of timolol (14.4 ± 1.1 g/kg/30 min, $P < 0.01$, Newman–Keuls *post hoc* test). No significant effect was observed in the rats injected with timolol alone (16.3 ± 1.6 g/kg/30 min), compared to the vehicle-injected rats (15.5 ± 1.5 g/kg/30 min).

3.3. Effect of intra-vBNST injection of isoproterenol on anxiety-like behaviors in the EPM test

To investigate β-adrenergic neurotransmission within the vBNST related to anxiety-like behaviors, we examined the effect of intra-vBNST isoproterenol injection in an EPM test. Intra-vBNST isoproterenol injection reduced the time spent in open arms in a dose-dependent manner (Fig. 4A). One-way ANOVA indicated a significant difference among groups ($F_{2, 32} = 4.90$, $P < 0.05$), and *post hoc* comparisons by Newman–Keuls test showed that isoproterenol at a dose of 30 nmol/side significantly decreased the time spent in open arms (50.0 ± 13.0 s, $P < 0.05$) compared to the vehicle-injected group (135.4 ± 21.4 s). Intra-vBNST injection of isoproterenol did not affect the number of closed arm entries in the EPM test (Fig. 4B; $F_{2, 32} = 1.06$, $P > 0.05$, one-way ANOVA), suggesting no effect of intra-vBNST isoproterenol injection on locomotor activity.

Off-site control injections of isoproterenol (30 nmol/side) into the lateral ventricle did not show any significant effect in the EPM test (Fig. 4C, D). Specifically, the time spent in open arms of the

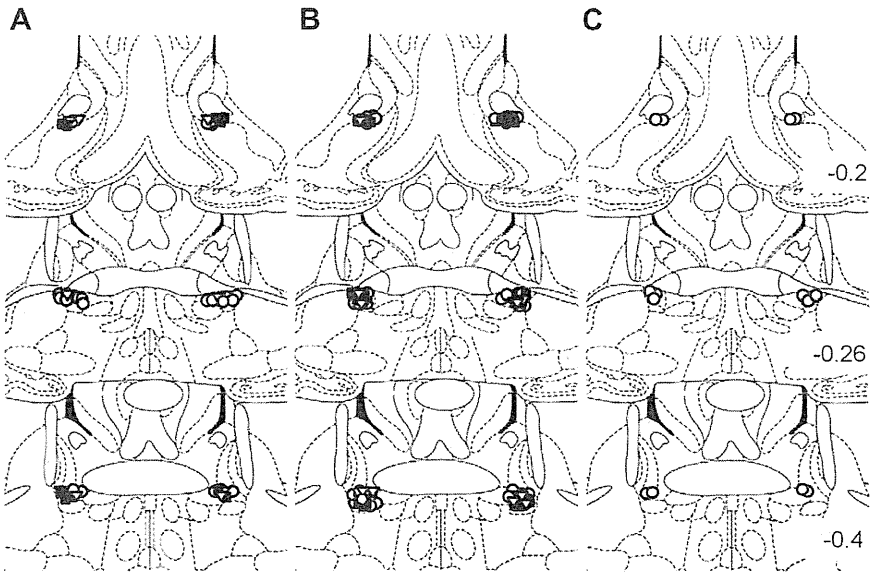

Fig. 1. Illustrations demonstrating the placement of the tips of microinjection cannulae in the food consumption test (A), EPM test (B), and rotarod test (C). (A) 10 nmol isoproterenol: open circles; 10 nmol timolol: open triangles; 10 nmol isoproterenol plus 10 nmol timolol: filled squares. (B) 30 nmol isoproterenol: open circles; 30 nmol timolol: open triangles; 30 nmol isoproterenol plus 30 nmol timolol: filled squares. (C) 30 nmol isoproterenol: open circles. The illustrations of coronal sections were taken from the atlas of Paxinos and Watson (1998); 0.2, −0.26, and −0.4 indicate distances (mm) from bregma.

isoproterenol-injected rats (70.9 ± 15.7 s) was not significantly ($P > 0.05$ ($P = 0.19$, $t = 1.38$), Student's *t*-test) different from that of the vehicle-injected group (109.0 ± 23.4 s). The number of closed arm entries was not different between the isoproterenol- and vehicle-injected rats ($P > 0.05$, Student's *t*-test).

3.4. Effect of co-administration of timolol on the anxiogenic effect of isoproterenol

The effect of co-administration of timolol on isoproterenol-induced anxiety-like behaviors in the EPM test was examined (Fig. 5). Two-way ANOVA indicated a significant main effect of isoproterenol ($F_{1, 48} = 18.1$, $P < 0.001$) and a significant interaction between the effects of isoproterenol and timolol ($F_{1, 48} = 6.65$; $P < 0.05$) on the time spent in open arms (Fig. 5A), but not on the number of closed arm entries (main effect of isoproterenol; $F_{1, 48} = 3.75$; $P > 0.05$) (Fig. 5B). The isoproterenol-induced reduction of the time spent in open arms (54.3 ± 11.4 s) was significantly reversed by the co-administration of timolol (127.0 ± 13.4 s, $P < 0.05$, Newman–Keuls *post hoc* test). No significant effect was observed in the rats injected with timolol alone (163.7 ± 34.6 s), compared to the vehicle-injected rats (203.9 ± 26.4 s).

3.5. Effect of intra-vBNST injection of isoproterenol on coordinated motor function in the rotarod test

The effect of intra-vBNST isoproterenol injection on motor function was determined using a rotarod test (Fig. 6). Rats that were bilaterally injected with isoproterenol (30 nmol/side) showed no

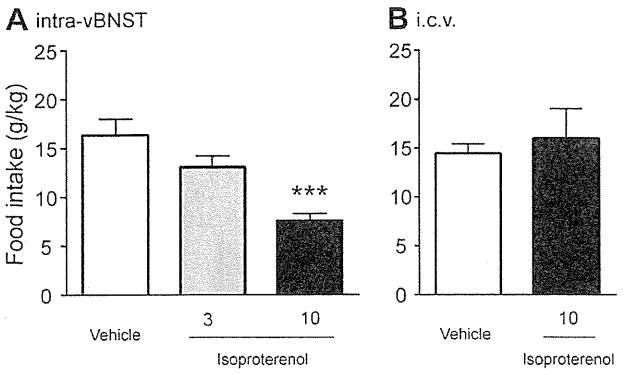

Fig. 2. The effect of intra-vBNST injection of isoproterenol on food intake in food-deprived rats. (A) The columns show food intake for 30 min after the injection of vehicle ($n = 5$) or isoproterenol (3 nmol, $n = 8$; 10 nmol, $n = 6$) into the vBNST. (B) The columns show food intake for 30 min after the injection of vehicle ($n = 6$) or isoproterenol (10 nmol, $n = 5$) into the lateral ventricle. Data are expressed as means ± SEM. ***$P < 0.001$ compared to the vehicle-injected rats (Newman–Keuls *post hoc* test).

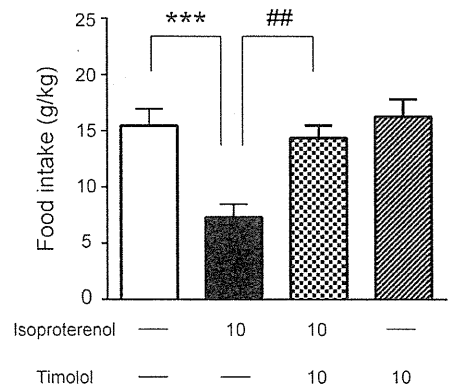

Fig. 3. The effect of co-administration of timolol on the reduction of food intake by isoproterenol. The columns show food intake for 30 min after the injection of vehicle ($n = 9$), 10 nmol/side isoproterenol ($n = 7$), 10 nmol/side isoproterenol plus 10 nmol/side timolol ($n = 7$), or 10 nmol/side timolol ($n = 7$). Data are expressed as means ± SEM. ***$P < 0.001$ compared to the vehicle-injected rats; ##$P < 0.01$ compared to the isoproterenol-injected rats (Newman–Keuls *post hoc* test).

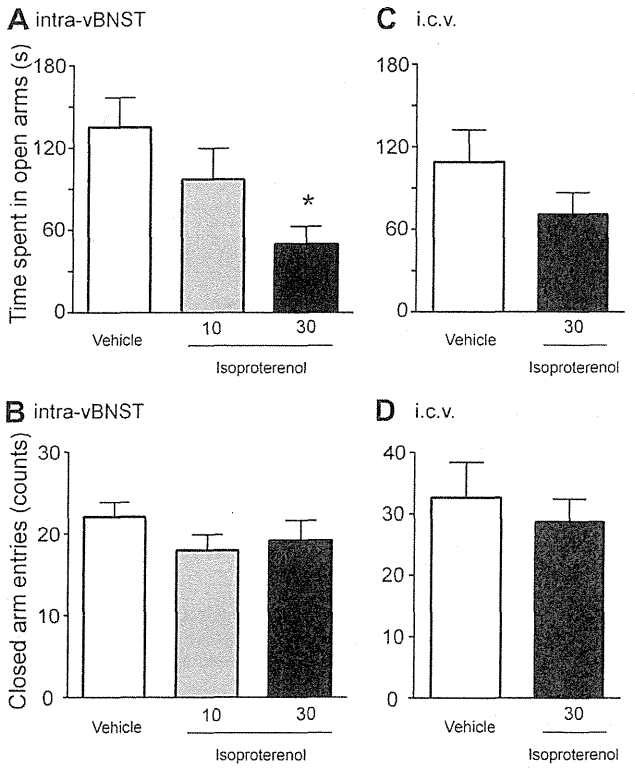

Fig. 4. The effect of intra-vBNST injection of isoproterenol on anxiety-like behaviors in the EPM test. (A, B) The columns show the time spent in open arms (A) and the number of closed arm entries (B) in rats injected with vehicle ($n = 15$) or isoproterenol (10 nmol, $n = 9$; 30 nmol, $n = 11$) into the vBNST. (C, D) The columns show the time spent in open arms (C) and the number of closed arm entries (D) in rats intracerebroventricularly injected with vehicle ($n = 9$) or isoproterenol (30 nmol, $n = 10$). Data are expressed as means ± SEM. $^{*}P < 0.05$ compared to the vehicle-injected rats (Newman–Keuls *post hoc* test).

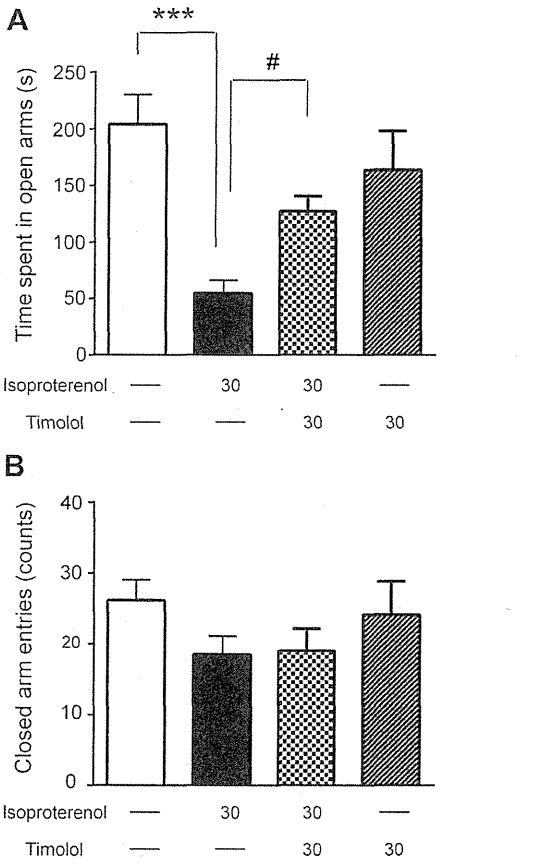

Fig. 5. The effect of co-administration of timolol on the anxiogenic effect of isoproterenol. The columns show the time spent in open arms (A) and the number of closed arm entries (B) in rats injected with vehicle ($n = 14$), 30 nmol/side isoproterenol ($n = 13$), 30 nmol/side isoproterenol plus 30 nmol/side timolol ($n = 15$), or 30 nmol/side timolol ($n = 10$). Data are expressed as means ± SEM. $^{***}P < 0.001$ compared to the vehicle-injected rats; $^{\#}P < 0.05$ compared to the isoproterenol-injected rats (Newman–Keuls post hoc test).

significant difference in the time spent on the rod compared to the vehicle-injected animals ($P > 0.05$, Student's *t*-test).

4. Discussion

Using food consumption and EPM tests, the present study demonstrates that intra-vBNST injection of isoproterenol, a β-adrenoceptor agonist, induced reduction of food intake and anxiety-like behaviors. Although behavioral tests can be affected by alterations in locomotor activity and motor function, the data of closed arm entries in the EPM test and the time spent on the rod in the rotarod test revealed that locomotor activity and motor function were not affected by intra-vBNST isoproterenol. Off-site control injections of isoproterenol into the lateral ventricle did not show any significant effect in the food consumption and EPM tests, suggesting that the vBNST is the likely site of action of isoproterenol although the contribution of bordering regions, including the dorsal BNST cannot be ruled out.

Important roles of intra-BNST noradrenergic transmission in negative emotional states have been reported. Fendt et al. (2005) reported that exposure to trimethylthiazoline, a component of fox odor, increased noradrenaline release in the BNST, and that intra-BNST administration of clonidine, an α_2-adrenoceptor agonist, suppressed both noradrenaline release and trimethylthiazoline-induced freezing behaviors. Delfs et al. (2000) reported that microinjection of β-antagonists or an α_2-agonist into the BNST markedly attenuated opiate withdrawal-induced CPA in rats. We previously demonstrated that intraplantar formalin- and intraperitoneal acetic acid-induced noxious stimuli increased noradrenaline release in the vBNST, and that intra-vBNST administration of timolol, a β-adrenoceptor antagonist, suppressed pain-induced CPA (Deyama et al., 2008, 2009). In addition, we recently reported that intra-vBNST injection of clonidine suppressed both pain-induced

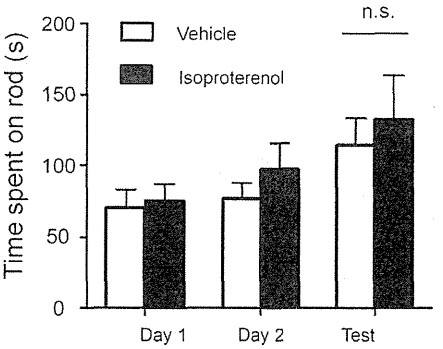

Fig. 6. The effect of intra-vBNST injection of isoproterenol on coordinated motor function in the rotarod test. The columns show the time spent on the rod in the rats injected with vehicle ($n = 9$) or 30 nmol/side isoproterenol ($n = 7$) on the test day. Data are expressed as means ± SEM.

noradrenaline release and CPA (Deyama et al., 2011). We also demonstrated that intra-vBNST injection of isoproterenol induced aversive responses in the CPA test (Deyama et al., 2008). These findings strongly suggest a pivotal role of intra-vBNST noradrenergic transmission via β-adrenoceptors in negative affective states. Our current study extends those findings by showing that intra-vBNST injection of isoproterenol induced anxiety-like behaviors in an EPM test.

We previously demonstrated that intra-vBNST injection of ICI118551, a β_2-adrenoceptor antagonist, significantly suppressed pain-induced aversive behaviors in a CPA test. However, betaxolol, a β_1-adrenoceptor antagonist, attenuated the aversive behaviors, but it was only a partial effect even at a high dose. Recently, Hott et al. (2012) reported that freezing behaviors in the conditioned contextual fear paradigm was suppressed by CGP20712, a β_1-adrenoceptor antagonist, but not by ICI118551. These findings suggest the differential contributions of β_1- and β_2-adrenoceptors to distinct emotional states. Further studies are needed to clarify the contributions of β_1- and β_2-adrenoceptors to reduced food intake and anxiety-like behaviors induced by intra-vBNST injection of isoproterenol.

Food intake is often suppressed by various kinds of stresses. However, we are only beginning to understand the mechanisms underlying the negative regulation of food intake by stresses. Reportedly, corticotropin-releasing factor (CRF), one of the key stress-response molecules, is involved in restraint stress- or emotional stress-induced inhibition of food intake (Sekino et al., 2004). Ciccocioppo et al. (2001) demonstrated that reduction of food intake by restraint stress or intracerebroventricular injection of CRF was attenuated by nociceptin. They also showed that reduction of food intake by CRF was reversed by intra-BNST injection of nociceptin, suggesting that the BNST is a neuroanatomical substrate for the suppressive effect of CRF on food intake and for its reversal by nociceptin (Ciccocioppo et al., 2003). In the present study, we found that intra-vBNST injection of a β-agonist, isoproterenol, suppressed food intake. This suggests that intra-BNST noradrenaline, another key molecule for stress responses in addition to CRF, plays an important role in the regulation of food intake.

The current study demonstrates that activation of β-adrenoceptors within the vBNST induces reduction of food intake and anxiety-like behaviors. In addition to the suppressive effect on food intake (Ciccocioppo et al., 2001, 2003), CRF induces anxiety-like behaviors in the EPM test when injected into the BNST (Sahuque et al., 2006). These findings suggest that the BNST is one of the neuroanatomical substrates which may be involved in the close relationship between negative affective states and reduction of food intake, and that two major stress-related molecules, noradrenaline and CRF, within this brain region play a critical role in inducing anxiety-like behaviors and reduced food intake.

Acknowledgments

This study was supported by a grant for Interdisciplinary Project for Psychosomatological Research in Hokkaido University, a Grant-in-Aid for Scientific Research (B) from the Japan Society for the Promotion of Science (JSPS) (M.M., 23300130), a Grant-in-Aid for Young Scientists (B) from JSPS (S.I., 22790239), and grants from the Hoansha Foundation (M.M.) and Naito Foundation (M.M.).

References

Ciccocioppo, R., Fedeli, A., Economidou, D., Policani, F., Weiss, F., Massi, M., 2003. The bed nucleus is a neuroanatomical substrate for the anorectic effect of corticotropin-releasing factor and for its reversal by nociceptin/orphanin FQ. J. Neurosci. 23, 9445–9451.

Ciccocioppo, R., Martin-Fardon, R., Weiss, F., Massi, M., 2001. Nociceptin/orphanin FQ inhibits stress- and CRF-induced anorexia in rats. Neuroreport 12, 1145–1149.

Delfs, J.M., Zhu, Y., Druhan, J.P., Aston-Jones, G., 2000. Noradrenaline in the ventral forebrain is critical for opiate withdrawal-induced aversion. Nature 403, 430–434.

Deyama, S., Ide, S., Kondoh, N., Yamaguchi, T., Yoshioka, M., Minami, M., 2011. Inhibition of noradrenaline release by clonidine in the ventral bed nucleus of the stria terminalis attenuates pain-induced aversion in rats. Neuropharmacology 61, 156–160.

Deyama, S., Katayama, T., Kondoh, N., Nakagawa, T., Kaneko, S., Yamaguchi, T., Yoshioka, M., Minami, M., 2009. Role of enhanced noradrenergic transmission within the ventral bed nucleus of the stria terminalis in visceral pain-induced aversion in rats. Behav. Brain Res. 197, 279–283.

Deyama, S., Katayama, T., Ohno, A., Nakagawa, T., Kaneko, S., Yamaguchi, T., Yoshioka, M., Minami, M., 2008. Activation of the β-adrenoceptor-protein kinase A signaling pathway within the ventral bed nucleus of the stria terminalis mediates the negative affective component of pain in rats. J. Neurosci. 28, 7728–7736.

Fendt, M., Siegl, S., Steiniger-Brach, B., 2005. Noradrenaline transmission within the ventral bed nucleus of the stria terminalis is critical for fear behavior induced by trimethylthiazoline, a component of fox odor. J. Neurosci. 25, 5998–6004.

Forray, M.I., Gysling, K., Andres, M.E., Bustos, G., Araneda, S., 2000. Medullary noradrenergic neurons projecting to the bed nucleus of the stria terminalis express mRNA for the NMDA-NR1 receptor. Brain Res. Bull. 52, 163–169.

Godart, N.T., Flament, M.F., Lecrubier, Y., Jeammet, P., 2000. Anxiety disorders in anorexia nervosa and bulimia nervosa: co-morbidity and chronology of appearance. Eur. Psychiatry 15, 38–45.

Hott, S.C., Gomes, F.V., Fabri, D.R., Reis, D.G., Crestani, C.C., Correa, F.M., Resstel, L.B., 2012. Both α_1- and β_1-adrenoceptors in the bed nucleus of the stria terminalis are involved in the expression of conditioned contextual fear. Br. J. Pharmacol. 167, 207–221.

Paxinos, G., Watson, C., 1998. The Rat Brain in Stereotaxic Coordinates, fourth ed. Academic Press, San Diego.

Pollice, C., Kaye, W.H., Greeno, C.G., Weltzin, T.E., 1997. Relationship of depression, anxiety, and obsessionality to state of illness in anorexia nervosa. Int. J. Eat. Disord. 21, 367–376.

Sahuque, L.L., Kullberg, E.F., McGeehan, A.J., Kinder, J.R., Hicks, M.P., Blanton, M.G., Janak, P.H., Olive, M.F., 2006. Anxiogenic and aversive effects of corticotropin-releasing factor (CRF) in the bed nucleus of the stria terminalis in the rat: role of CRF receptor subtypes. Psychopharmacology (Berl) 186, 122–132.

Sekino, A., Ohata, H., Mano-Otagiri, A., Arai, K., Shibasaki, T., 2004. Both corticotropin-releasing factor receptor type 1 and type 2 are involved in stress-induced inhibition of food intake in rats. Psychopharmacology (Berl) 176, 30–38.

Walker, D.L., Toufexis, D.J., Davis, M., 2003. Role of the bed nucleus of the stria terminalis versus the amygdala in fear, stress, and anxiety. Eur. J. Pharmacol. 463, 199–216.

Woulfe, J.M., Flumerfelt, B.A., Hrycyshyn, A.W., 1990. Efferent connections of the A1 noradrenergic cell group: a DBH immunohistochemical and PHA-L anterograde tracing study. Exp. Neurol. 109, 308–322.

Behavioral/Cognitive

Opposing Roles of Corticotropin-Releasing Factor and Neuropeptide Y within the Dorsolateral Bed Nucleus of the Stria Terminalis in the Negative Affective Component of Pain in Rats

Soichiro Ide,[1] Taiki Hara,[1] Atsushi Ohno,[1] Ryuta Tamano,[1] Kana Koseki,[1] Tomonori Naka,[1] Chikashi Maruyama,[1] Katsuyuki Kaneda,[1] Mitsuhiro Yoshioka,[2] and Masabumi Minami[1]

[1]Department of Pharmacology, Graduate School of Pharmaceutical Sciences, Hokkaido University, Sapporo 060-0812, Japan and [2]Department of Neuropharmacology, Graduate School of Medicine, Hokkaido University, Sapporo 060-8638, Japan

Pain is a complex experience composed of sensory and affective components. Although the neural systems of the sensory component of pain have been studied extensively, those of its affective component remain to be determined. In the present study, we examined the effects of corticotropin-releasing factor (CRF) and neuropeptide Y (NPY) injected into the dorsolateral bed nucleus of the stria terminalis (dlBNST) on pain-induced aversion and nociceptive behaviors in rats to examine the roles of these peptides in affective and sensory components of pain, respectively. *In vivo* microdialysis showed that formalin-evoked pain enhanced the release of CRF in this brain region. Using a conditioned place aversion (CPA) test, we found that intra-dlBNST injection of a CRF_1 or CRF_2 receptor antagonist suppressed pain-induced aversion. Intra-dlBNST CRF injection induced CPA even in the absence of pain stimulation. On the other hand, intra-dlBNST NPY injection suppressed pain-induced aversion. Coadministration of NPY inhibited CRF-induced CPA. This inhibitory effect of NPY was blocked by coadministration of a Y_1 or Y_5 receptor antagonist. Furthermore, whole-cell patch-clamp electrophysiology in dlBNST slices revealed that CRF increased neuronal excitability specifically in type II dlBNST neurons, whereas NPY decreased it in these neurons. Excitatory effects of CRF on type II dlBNST neurons were suppressed by NPY. These results have uncovered some of the neuronal mechanisms underlying the affective component of pain by showing opposing roles of intra-dlBNST CRF and NPY in pain-induced aversion and opposing actions of these peptides on neuronal excitability converging on the same target, type II neurons, within the dlBNST.

Introduction

Pain is a complex experience consisting of sensory and affective components. Although the neural systems of the sensory component of pain have been studied extensively, those of the negative affective component are only beginning to be understood. Recently, some behavioral studies using a conditioned place paradigm have revealed neural mechanisms underlying the negative affective component of pain. Johansen et al. (2001) reported the crucial role of the anterior cingulate cortex in conditioned place aversion (CPA) induced by the intraplantar injection of formalin. We reported that the central amygdaloid nucleus and basolateral amygdaloid nucleus (BLA) were differently involved in intraplantar formalin-induced and intraperitoneal acetic acid-induced CPA (Tanimoto et al., 2003). In addition to these brain areas, we found that the excitotoxic lesions of the bed nucleus of the stria terminalis (BNST) reduced pain-induced aversion without reducing nociceptive behaviors (Deyama et al., 2007). Moreover, we recently demonstrated that noradrenergic neurotransmission within the ventral part of BNST mediated the negative affective component of pain (Deyama et al., 2008, 2009, 2011).

The dorsolateral part of the BNST (dlBNST) is densely innervated with corticotropin-releasing factor (CRF)-containing fibers (Sakanaka et al., 1986; Morin et al., 1999) and expresses CRF receptors (Van Pett et al., 2000). Intra-BNST CRF has been implicated in negative affective states, such as anxiety, fear, and aversion. Intra-BNST infusion of CRF has been shown to elicit anxiety-associated behaviors in the elevated plus maze test (Sahuque et al., 2006) and to enhance startle responses (Lee and Davis, 1997). Furthermore, it has been reported that intra-BNST administration of CRF produced CPA (Sahuque et al., 2006). However, the role of CRF-mediated neurotransmission within the dlBNST in the negative affective component of pain remains unclear.

Received Sept. 7, 2012; revised Jan. 30, 2013; accepted Feb. 7, 2013.

Author contributions: K. Kaneda, M.Y., and M.M. designed research; S.I., T.H., A.O., R.T., K. Koseki, T.N., and C.M. performed research; S.I., K. Kaneda, and M.M. analyzed data; S.I., K. Kaneda, and M.M. wrote the paper.

This study was supported by a grant for Interdisciplinary Project for Psychosomatological Research in Hokkaido University; a Grant-in-Aid for Scientific Research (B) from the Japan Society for the Promotion of Science (JSPS) (M.M., 23300130); a Grant-in-Aid for Young Scientists (B) from JSPS (S.I., 22790239); Health Labour Sciences Research Grant (research on chronic pain) from the Ministry of Health, Labour, and Welfare (M.M.); and grants from the Hoansha Foundation (M.M.) and Naito Foundation (M.M.).

The authors declare no competing financial interests.

Correspondence should be addressed to Masabumi Minami, Department of Pharmacology, Graduate School of Pharmaceutical Sciences, Hokkaido University, Sapporo 060-0812, Japan. E-mail: mminami@pharm.hokudai.ac.jp.

DOI:10.1523/JNEUROSCI.4278-12.2013

 0270-6474/13/335881-14$15.00/0

Neuropeptide Y (NPY)-containing fibers are also observed in the dlBNST (Walter et al., 1991), and its receptors, Y_1, Y_2, Y_4, and Y_5 subtypes, are expressed in this brain region (Parker and Herzog, 1999). Although a large body of literature exists on the anxiolytic and anti-aversive effects of NPY (Heilig, 1995; Kask et al., 1997; Nakajima et al., 1998; Gutman et al., 2008), the role of this peptide in pain-induced aversion remains to be determined.

In this study, we examined the effects of intra-dlBNST injection of CRF and NPY on pain-induced aversion and nociceptive behaviors to examine the roles of these peptides in affective and sensory components of pain, respectively, and revealed their opposing roles in the negative affective component of pain. Furthermore, whole-cell patch-clamp electrophysiology in dlBNST slices showed opposing actions of these peptides on neuronal excitability specifically in type II dlBNST neurons.

Materials and Methods

Animals. Male Sprague Dawley rats (Japan SLC) (180–280 g or 20 to 50 d old) were used for the behavioral or electrophysiological experiments, respectively. The rats were maintained at a constant ambient temperature (22 ± 1°C) under a 12 h light/dark cycle with food and water available *ad libitum*. All experiments were performed with the approval of the Institutional Animal Care and Use Committee at Hokkaido University.

Drugs. NBI27914 (a selective CRF_1 receptor antagonist), antisauvagine-30 (AS-30; a selective CRF_2 receptor antagonist), and L-152,804 (a selective NPY Y_5 receptor antagonist) were purchased from Tocris Bioscience. CRF was purchased from Peptide Institute or Bachem AG. NPY and BIBP3226 (a selective NPY Y_1 antagonist) were from Abgent and Bachem AG, respectively. Tetrodotoxin (TTX) was from Wako Pure Chemical Industries and SR95531, ZD7288, and kynurenic acid were from Sigma.

For the behavioral experiments, AS-30 was dissolved in PBS, pH 7.4, containing 0.1% bovine serum albumin (BSA; Sigma). NBI27914 was dissolved in dimethylsulfoxide (DMSO), then diluted with PBS containing 0.1% BSA; the solution contained DMSO at a final concentration of 8.4%. The final concentration of these antagonists was 0.3 nmol/0.5 μl or 1.0 nmol/0.5 μl. NPY was dissolved in PBS containing 0.1% BSA at a concentration of 0.1 nmol/0.5 μl or 0.3 nmol/0.5 μl. CRF was dissolved in saline containing 0.1% BSA and 0.03% acetic acid, then mixed with PBS containing 0.1% BSA at a ratio of 2:1. The final concentration of CRF was 0.1 nmol/0.6 μl or 0.3 nmol/0.6 μl. When the effects of NPY in the presence or absence of NPY antagonists on CRF-induced CPA were examined, CRF solution was mixed with these drugs dissolved in PBS containing 0.1% BSA at a ratio of 2:1. L-152,804 was dissolved in DMSO, then diluted with PBS containing 0.1% BSA; the solution contained DMSO at a final concentration of 16.7%.

For the electrophysiological experiments, the stock solutions for CRF and NPY were prepared at concentrations of 1 mM in H_2O containing 0.1% BSA. The stock solutions for NBI27914 and AS-30 were prepared at a concentration of 300 μM in DMSO and in H_2O containing 0.1% BSA, respectively. The stock solutions for BIBP3226 and L-152,804 were prepared at a concentration of 1 mM in H_2O and in DMSO, respectively. The stock solution for ZD7288 was prepared at a concentration of 10 mM in H_2O. These stock solutions were stored at –30°C until use. Before bath application, these stock solutions were diluted to final concentrations with normal Ringer's solution containing 0.01% BSA. We confirmed that bath application of DMSO alone at the final concentration (0.1%) did not affect either membrane potential or input resistance (data not shown).

In vivo *microdialysis. In vivo* microdialysis was performed using a peptide microdialysis system (AtmosLM; Eicom). Under sodium pentobarbital anesthesia (50 mg/kg, i.p.), each rat was implanted unilaterally with a microdialysis guide cannula (outer diameter, o.d.; 0.72 mm, PEG-6; Eicom) 1.0 mm above the dlBNST (–0.3 mm rostral, 1.7 mm lateral, 5.5 mm ventral to bregma) (Paxinos and Watson, 1998). After surgery, rats were housed individually in cages. One day after the implantation of the guide cannula, microdialysis experiments were performed in unanesthetized and freely moving rats. Microdialysis probes (dialysis membrane: 1000 kDa molecular weight cutoff polyethylene membrane, length 1.0 mm; o.d., 0.44 mm; PEP-6–01; Eicom) were inserted through the guide cannula and continuously perfused with Ringer's solution (Na^+ 147 mM, K^+ 4 mM, Ca^{2+} 2.3 mM, and Cl^- 155.6 mM) containing 0.15% BSA at a flow rate of 10 μl /min. The rats were then placed in a Plexiglas chamber (30 × 30 × 35 cm: width × length × height) for the 2 h preconditioning period. After the preconditioning period, the flow rate was changed to 1 μl/min. After an additional stabilization period of 1 h, 11 15 min dialysates were collected in polypropylene tubes at 4°C. The first three samples were taken as baseline samples. Immediately after collection of the last baseline sample, each rat was administered an intraplantar injection (right hindpaw) of 100 μl of 2% formalin. Dialysate samples were stored at –20°C. CRF concentrations in the samples were measured using a competitive enzyme immunoassay kit (Phoenix Pharmaceuticals).

Surgery and microinjection. Under sodium pentobarbital anesthesia (50 mg/kg, i.p.), rats were implanted bilaterally with 25 gauge stainless steel guide cannulae (o.d., 0.5 mm; inner diameter, i.d., 0.22 mm) 1.5 mm above the dlBNST (–0.3 mm rostral, 1.7 mm lateral, 5.0 mm ventral to bregma) or lateral ventricle (–0.3 mm rostral, 1.4 mm lateral, 2.7 mm ventral to bregma) (Paxinos and Watson, 1998). After surgery, rats were housed individually in plastic cages with woodchip bedding, allowed to recover for at least 5 d, and handled for 1–2 min each day for 3 consecutive days before behavioral experiments. For microinjection, 33 gauge stainless steel injection cannulae (o.d., 0.2 mm; i.d., 0.08 mm) were inserted bilaterally into the guide cannulae. The injection cannulae protruded 1.5 mm from the tip of the guide cannulae to reach the dlBNST or lateral ventricle. Injection cannulae were attached to a microinjection pump (CMA) via PE 8 polyethylene tubing. Drug or vehicle was administrated bilaterally in a volume of 0.5–0.6 μl/side at a rate of 0.5 μl/min, and the injection cannulae were left in place for an additional 1 min after microinjection to prevent backflow.

Conditioned CPA. CPA tests were conducted as described previously (Deyama et al., 2007, 2008, 2009). A shuttle box composed of two equal-sized compartments (30 × 30 × 30 cm) with distinct visual and tactile cues (one compartment was black with a smooth floor, and the other was white with a textured floor) under dim illumination (25 ± 5 lux at the center of the box) was used for a 4 consecutive day experimental procedure. On day 1 (habituation session) and day 2 (preconditioning session), rats explored the two compartments *ad libitum* for 900 s; the time spent in each compartment during the exploring period was measured automatically (KN-80; Natsume Seisakusho). Rats that spent >80% (>720 s) of the total time (900 s) in one side on day 2 or showed a difference of >200 s in the time spent in one side between days 1 and 2 were eliminated from subsequent procedures. Additionally, after behavioral tests, histological analyses were performed, and data from rats with misplacement of both or either of the bilateral microinjection cannulae were eliminated from statistical analyses. Both before and after such eliminations, no significant difference ($p > 0.05$ ($n = 353$) and $p > 0.05$ ($n = 197$), respectively) was observed between the time spent in the black (442.6 ± 6.3 s and 445.8 ± 7.1 s, respectively) and white (457.4 ± 6.3 s and 454.2 ± 7.1 s, respectively) compartments, indicating the absence of any significant bias in compartment preference before conditioning.

Formalin-induced CPA was used to evaluate the affective component of pain (Johansen et al., 2001; Tanimoto et al., 2003; Johansen and Fields, 2004; Deyama et al., 2008, 2011). In this CPA test, we used a bias-like protocol (Tzschentke, 1998). Specifically, we designated the compartment in which each rat spent more time (>450 s) on day 2 (preconditioning session) as each animal's pain-paired compartment. This type of protocol was successfully used to examine the CPA induced by opioid withdrawal (Kosten, 1994; Rafieian-Kopaei et al., 1995; Nakagawa et al., 2005) and by visceral and somatic pain (Tanimoto et al., 2003; Deyama et al., 2007, 2008, 2009). On day 3 (conditioning session), place conditioning was performed as follows. In the vehicle control session (conducted between 08:00 and 12:00), each rat was given an intraplantar injection of saline (100 μl) into the left hindpaw and then immediately confined in the nonpain-paired compartment for 1 h. After at least 4 h, in the pain-conditioning session (conducted between 14:00 and 18:00), each rat was injected with NBI27914 (0.3 nmol/side or 1 nmol/side), AS-30 (0.3 nmol/side or 1 nmol/side), NPY (0.1 nmol/side or 0.3 nmol/side), or

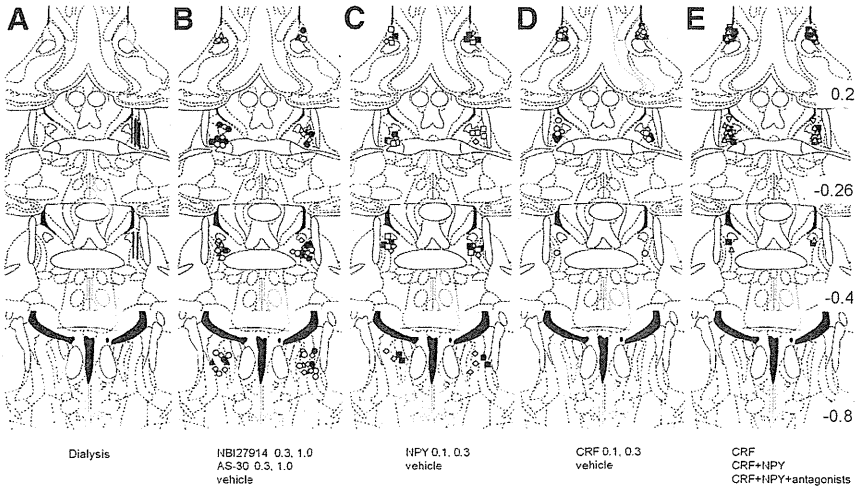

Figure 1. The placements of the tips of the microdialysis probes (***A***) and microinjection cannulae (***B–E***). ***B***, NBI27914 1.0 nmol, closed circles; 0.3 nmol, open circles; AS-30 1.0 nmol, closed triangles; 0.3 nmol, open triangles; vehicle, open rhomboids. ***C***, NPY 0.3 nmol, closed squares; 0.1 nmol, open squares; vehicle, open rhomboids. ***D***, CRF 0.3 nmol, closed circles; 0.1 nmol, open circles; vehicle, open rhomboids. ***E***, CRF, closed circles; CRF+NPY, closed squares; CRF+NPY+BIBP3226, open reversed triangles; CRF+NPY+ L-152,804, open triangles. The illustrations of coronal sections were taken from the atlas of Paxinos and Watson (1998); 0.2, −0.26, −0.4, and −0.8 indicate distances (mm) from bregma.

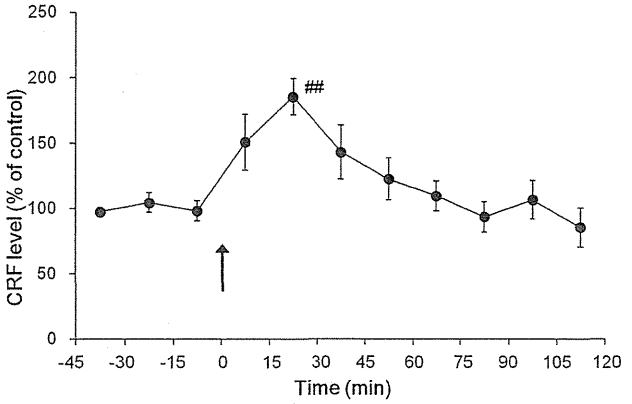

Figure 2. Effects of intraplantar injection of formalin ($n = 7$) on extracellular CRF levels in the dlBNST were examined. The arrow indicates the time point of intraplantar injection. Data are expressed as means ± SEM the percentage baseline control value, calculated as an average of three consecutive dialysates before intraplantar injection. $^{\#\#}p < 0.01$ compared with the value just before intraplantar injection (Newman–Keuls *post hoc* test).

vehicle into the bilateral dlBNST or lateral ventricle. At 10 min after the intra-dlBNST injection, the rats were given an intraplantar injection of 2% formalin (100 μl) into the right hindpaw and then confined in the pain-paired compartment for 1 h. On day 4 (test session), each rat was allowed to explore the two compartments *ad libitum*, and the time spent in each compartment during the exploring period (900 s) was recorded automatically. CPA scores were calculated by subtracting the time spent in the pain-paired compartment during the test session from the time spent in this compartment during the preconditioning session.

In the experiments investigating intra-dlBNST CRF-induced aversion (a 6 consecutive day experimental protocol), we designated the compartment in which the rat spent more time (>450 s) on day 2 (preconditioning session) as the drug-paired compartment for each animal. On days 3–5, place conditioning was performed over 3 consecutive days as follows. The rats were divided into two groups (Groups 1 and 2). In the morning session (conducted between 08:00 and 12:00), rats in Group 1 were given an intra-dlBNST injection of drugs or vehicle and were immediately confined in the drug-paired compartment for 30 min. On the other hand, rats in Group 2 were confined in the nondrug-paired compartment for 30 min without being given an intra-dlBNST injection. In the afternoon session (conducted between 13:00 and 18:00), rats in Group 1 were confined in the nondrug-paired compartment for 30 min without being given an intra-dlBNST injection, and rats in Group 2 were given an intra-dlBNST injection of drugs or vehicle and were immediately confined in the drug-paired compartment for 30 min. On day 6, in the test session, each rat was allowed to explore the two compartments freely, and the time spent in each compartment during the exploring period (900 s) was recorded. CPA scores were calculated as in the CPA test for pain-induced aversion.

Formalin test. Formalin-induced nociceptive behaviors were examined to evaluate the sensory component of pain (Johansen et al., 2001; Tanimoto et al., 2003; Johansen and Fields, 2004; Deyama et al., 2008, 2011). Each rat was placed in a Plexiglas cylinder (30 cm diameter; 30 cm height) for 30 min to acclimatize it to the experimental environment. Drugs or vehicle were injected bilaterally into the dlBNST of each rat, and the animals were returned to the cylinder. At 10 min after the intra-dlBNST injection, the rats were given an intraplantar injection of 2% formalin (100 μl) into the right hindpaw and immediately returned to the cylinder. The amount of time the rat spent lifting, licking, shaking, or biting the injected paw was measured for each 5 min period over 60 min. Measurement of nociceptive behaviors was done live by an observer blind to the treatment conditions. Nociception was quantified using a rating scale method by assigning weights to the following categories of nociceptive behaviors: category 0 = weight is evenly distributed among all paws; category 1 = injected paw is lifted; and category 2 = injected paw is licked, shaken, or bitten. The nociceptive score was calculated for each 5 min (300 s) period using the following formula: nociceptive score = [{time (s) spent with lifting the injected paw} × 1 + {time (s) spent with licking, shaking, or biting the injected paw} × 2]/300 (s).

Histology. After the *in vivo* microdialysis experiments and behavioral tests, histological analyses were performed. Rats were decapitated, and brains were removed rapidly and frozen in powdered dry ice. Coronal sections (50 μm) including the BNST were prepared with a cryostat, thaw-mounted onto slides, stained with thionine, and examined under a microscope (×40). Data from the rats with extensive tissue damage, misplacement of the microdialysis probes, or misplacement of both or either of the bilateral injection cannulae were excluded from statistical analyses.

Slice preparation for electrophysiology. Rats were decapitated under isoflurane anesthesia, and the brains were quickly removed and submerged in ice-cold artificial CSF containing the following (in mM): 130 NaCl, 3.5 KCl, 1.1 KH_2PO_4, 1.0 $CaCl_2$, 6.0 $MgCl_2$, 30 $NaHCO_3$, 10 glucose, and 2 kynurenic acid, saturated with 95% O_2/5% CO_2. Coronal slices (250 μm thick) containing the BNST region were prepared using a microslicer (VT1200S; Leica). Slices were incubated in a chamber containing normal Ringer's solution containing the following (in mM): 125 NaCl, 2.5 KCl, 1.25 NaH_2PO_4, 2.0 $CaCl_2$, 1.0 $MgCl_2$, 26 $NaHCO_3$, and 25 glucose, saturated with 95% O_2/5% CO_2 at 33–35°C for 0.5 h, and then placed at room temperature for >0.5 h before recording.

Recording procedures for electrophysiology. Slices were placed in a recording chamber on an upright microscope (BX-51WI; Olympus) and continuously superfused with normal Ringer's solution (34°C) saturated with 95% O_2/5% CO_2 at a flow rate of 1–1.5 ml/min. Pipettes were pulled from thin-walled borosilicate glass capillaries with a micropipette puller (Model P-1000; Sutter Instrument). Tip resistance was 5–8 MΩ when pipettes were filled with an internal solution containing the following (in mM): 150 KOH, 2 $MgCl_2$, 10 KCl, 0.2 EGTA, 2 Na_2-ATP, 0.3 Na_2-GTP, 10 HEPES, and 0.1 spermine. The pH was adjusted to 7.3–7.4 with gluconic

acid. Recordings were obtained from dlBNST neurons visualized with infrared video microscopy (model IR-1000; Dage-MTI). Because dlBNST neurons have been categorized into three distinct types (Hammack et al., 2007), we first identified cell types by assessing the membrane potential responses to hyperpolarizing and depolarizing current injections. To monitor hyperpolarizing responses, we set the initial membrane potential at −60 mV and incremental currents (400 ms) ranging from 0 to −360 pA were injected. To monitor depolarizing and firing responses, we set the initial membrane potential at −80 mV, and incremental currents (400 ms) ranging from 0 to 160 pA were injected. Neurons that exhibited a depolarizing sag in response to hyperpolarizing current injection and a regular firing pattern in response to depolarizing current injection were classified as type I. Neurons that exhibited a depolarizing sag in response to hyperpolarizing current injection and burst firings in response to both the termination of the hyperpolarizing current injections and depolarizing current injections were classified as type II. Neurons that exhibited no depolarizing sag in response to hyperpolarizing current injection and a regular firing pattern in response to depolarizing current injection were classified as type III. Neurons were excluded from analyses if the amplitude of the action potential, which was determined as the difference between threshold and the peak, was <30 mV. Data were acquired with a Multiclamp 700B amplifier and the pClamp10 software (Molecular Devices).

Measurement of membrane potentials and input resistance. The initial membrane potentials were set to approximately –70 mV (−69.32 ± 0.23 mV, $n = 50$) by injecting negative or positive currents. To inhibit action potential-induced synaptic transmission, 500 nM TTX was added to superfused Ringer's solution. To monitor the changes in membrane potentials, a window with a 1 s duration was placed every 5 s, and the average membrane potential within the window was determined. To monitor changes in input resistance, input resistance was calculated by measuring the change in membrane potential evoked by a negative current (−80 pA, 200 ms) every 5 s. Then, the membrane potentials and input resistance during a 1 min period were calculated by averaging 12 of these values. After confirming stable membrane potentials and input resistance for >3 min, 1 μM CRF or 1 μM NPY was perfused through the recording chamber for 2 min except for the experiment shown in Figure 8, where NPY was perfused until the end of the experiment. In experiments assessing the effects of antagonists for CRF or NPY receptors on CRF- or NPY-induced change in membrane potentials, the antagonists were perfused for >10 min before bath application of CRF or NPY to the end of the experiments. Membrane potentials and input resistance were measured in the periods of 0–3 min before and 13–16 min after drug application. The latter period was chosen because the effects of CRF and NPY emerged gradually and became maximal in this period in most of the neurons tested. The effects of drugs were evaluated by comparing the average values observed during these two periods.

Analyses of steady-state membrane current–voltage relationships. Steady-state membrane current–voltage (*I–V*) relationships were examined in type II dlBNST neurons. Cells were voltage clamped at –70 mV in the presence of 1 μM TTX. To assess the *I–V* relationship, we used a voltage ramp protocol described in a previous study (Hara and Nakaya, 1997) with some modifications. Briefly, the membrane potential was first depolarized to 0 mV and then hyperpolarized to –120 mV at a rate of 0.1 mV/ms every 20 s. The current responses observed during the falling phase from –30 mV to –120 mV were used for *I–V* relationship analyses. Changes in net currents caused by a 2 min bath application of CRF or NPY were determined by subtracting the current responses to the voltage ramp in the periods of 0–3 min before drug application from those of 13–16 min after drug application. In some experiments, effects of NPY on *I–V* relationships were examined in the presence of ZD7288.

To measure holding currents, a window with a 1 s duration was placed every 20 s, and the average holding current within the window was determined. To monitor the changes in input resistance, input resistance was calculated by measuring the change in the holding current evoked by voltage steps (–5 mV, 30 ms) every 20 s. Holding currents and input resistance were measured in the periods of 0–3 min before and 13–16 min after drug application. The effects of drugs were evaluated by comparing the average values observed at these two periods.

Measurement of firing activity. To measure changes in firing activity, current-clamp recordings without current injection were carried out. To inhibit $GABA_A$ receptor-mediated and ionotropic glutamate receptor-mediated synaptic transmission, 10 μM SR95531 and 1 mM kynurenic

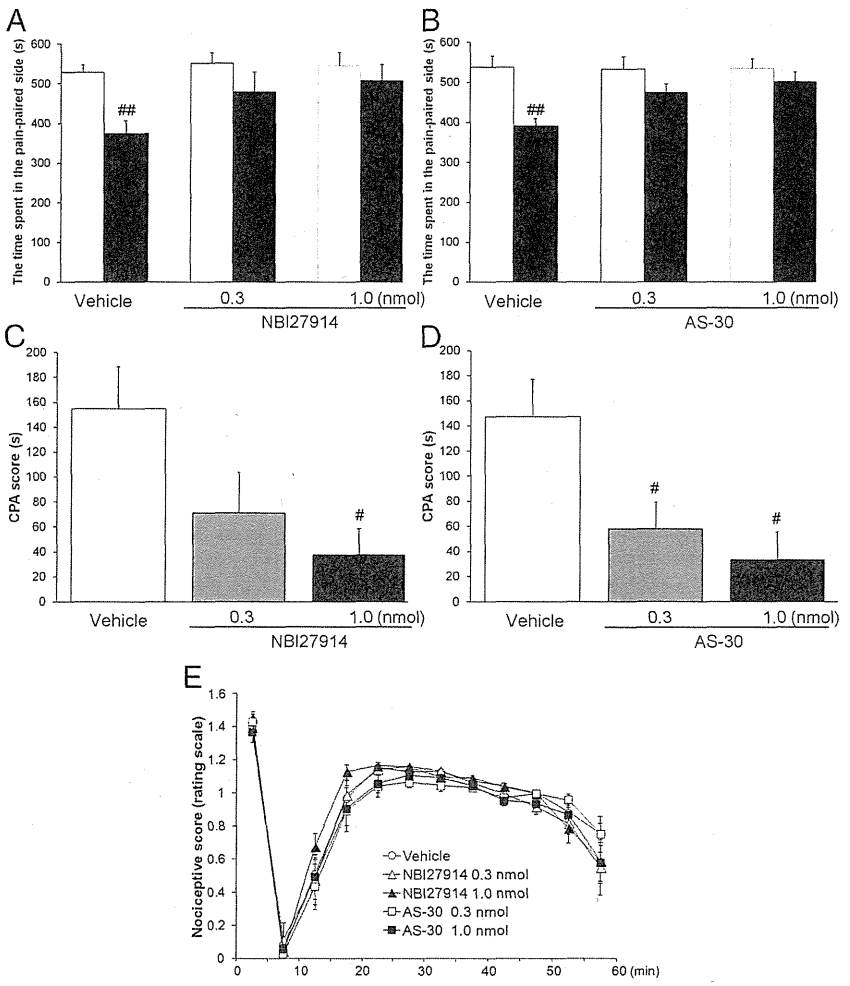

Figure 3. ***A–D***, Effects of intra-dlBNST injection of NBI27914 (***A***, ***C***, vehicle, $n = 7$; 0.3 nmol, $n = 8$; 1.0 nmol, $n = 7$) or AS-30 (***B***, ***D***, vehicle, $n = 6$; 0.3 nmol, $n = 6$; 1.0 nmol, $n = 7$) on formalin-induced CPA. Data are expressed as means ± SEM. The columns show the time spent in the pain-paired compartment in the preconditioning (white columns) and test (black columns) sessions (***A***, ***B***). $^{\#\#}p < 0.01$ compared with the preconditioning session (paired *t* test). The columns show the CPA scores (***C***, ***D***). $^{\#}p < 0.05$ compared with vehicle-injected rats (Newman–Keuls *post hoc* test). ***E***, Effects of intra-dlBNST injection of vehicle ($n = 11$), NBI27914 (0.3 nmol, $n = 6$; 1.0 nmol, $n = 7$), or AS-30 (0.3 nmol, $n = 6$; 1.0 nmol, $n = 6$) on formalin-induced nociceptive behaviors. Data are expressed as means ± SEM.

acid, respectively, were added to superfused Ringer's solution. To analyze firing activity, a window with 2.5 s duration was placed every 5 s, and the numbers of spikes in 36 windows were counted during 3 min. After counting basal firing activities, 1 μM CRF was perfused through the recording chamber for 2 min in the presence or absence of 1 μM NPY. NPY was perfused from 7.5 to 11 min before CRF application to the end of the experiments. Firing activities were measured during a period of 0–3 min before the application of peptides and 17–20 min after CRF application. The latter period was chosen because maximum firing activities were observed in this period in most of the neurons tested. The effects of drugs were evaluated by comparing the average values observed during these periods.

Statistical analyses. Data are expressed as means ± SEM. *In vivo* microdialysis data were assessed using one-way repeated-measures ANOVA followed by the Newman–Keuls *post hoc* test. Time spent in the pain- or drug-paired compartment during preconditioning and test sessions in the CPA test was analyzed using within-group paired *t* tests. CPA scores were analyzed using one-way ANOVA followed by the Newman–Keuls *post hoc* test or Student's *t* test for comparisons among more than two groups or between two groups, respectively. Two-way repeated-measures ANOVA was used for the data from measurements of nociceptive behaviors. Electrophysiological data were analyzed using the paired *t* test, Student's *t* test, or one-way repeated-measures ANOVA followed by the Newman–Keuls *post hoc* test. Statistical analyses were performed using IBM SPSS statistics v.20.0.0 or using GraphPad Prism v.6.00 (GraphPad Software); p values < 0.05 were considered to indicate statistically significant differences.

Results

Histology

After the *in vivo* microdialysis experiments and behavioral tests, histological analyses were performed. Data from rats with correct placements of the microdialysis probe (Fig. 1*A*) and of the bilateral microinjection cannulae (Fig. 1*B–E*) were used for the statistical analyses.

Pain-induced CRF release within the dlBNST

The averaged baseline concentration of CRF in the dialysates was 6.8 ± 0.5 pg/15 μl. Intraplantar injection of formalin produced a transient increase in extracellular CRF levels within the dlBNST (Fig. 2). One-way repeated-measures ANOVA demonstrated a significant effect of the formalin injection ($F_{(10,76)} = 4.50$, $p < 0.001$, $n = 7$). A significant increase in the CRF level was observed at 15–30 min after the formalin injection (186 ± 14%; $p < 0.01$ compared with the last baseline sample (−15 to 0 min), Newman–Keuls *post hoc* test).

Effects of intra-dlBNST injection of CRF receptor antagonists on formalin-induced CPA and nociceptive behaviors

To determine the role of CRF-mediated neurotransmission within the dlBNST in the affective component of pain, the effects of bilateral intra-dlBNST injection of NBI27914 (CRF_1 receptor antagonist) and AS-30 (CRF_2 receptor antagonist) on formalin-induced CPA were examined. In the intra-dlBNST vehicle-injected rats, the time spent in the pain-paired compartment during the test session (374 ± 33 and 391 ± 18 s in Fig. 3*A*,*B*, respectively) was significantly shorter ($t = 4.55$ (df = 6), $p < 0.01$ and $t = 4.91$ (df = 5), $p < 0.01$, respectively, paired *t* test) than the time during the preconditioning session (529 ± 19 and 538 ± 29 s). In the intra-dlBNST NBI27914 (0.3 and 1 nmol/side)-injected rats, no significant difference ($t = 2.19$ (df = 7), $p > 0.05$ and $t = 1.82$ (df = 6), $p > 0.05$, respectively, paired *t* test) was observed in the time spent in the pain-paired compartment between the test (480 ± 50 and 508 ± 41 s, respectively) and the preconditioning (551 ± 28 and 546 ± 32 s, respectively) sessions.

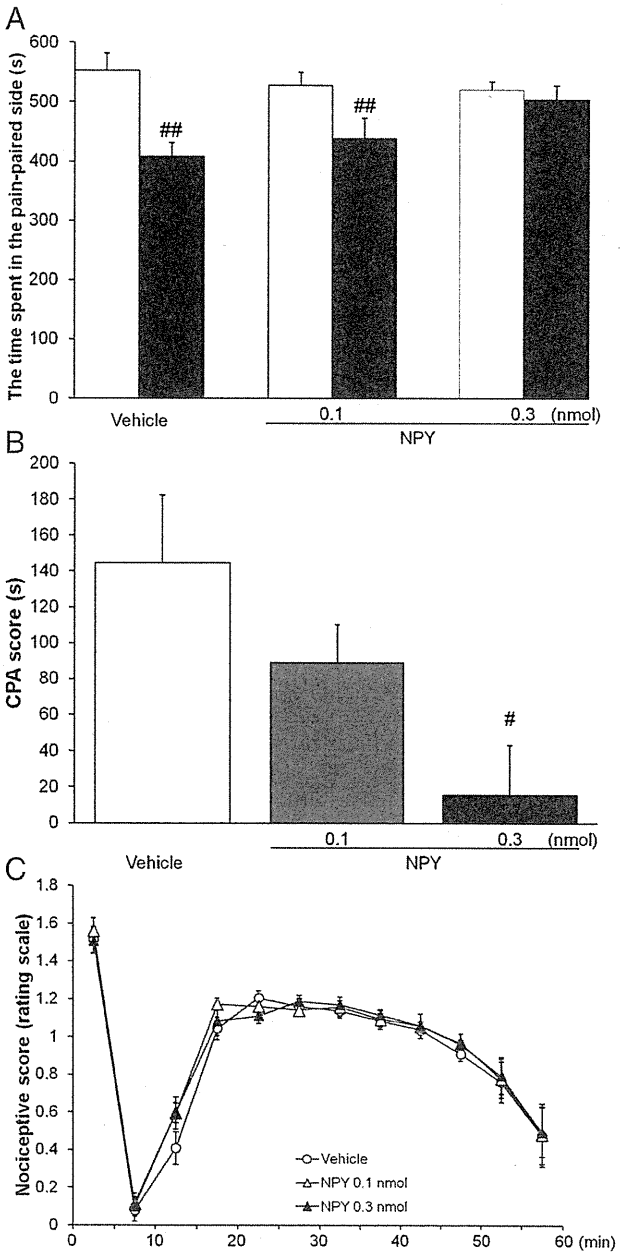

Figure 4. *A*, *B*, Effects of intra-dlBNST injection of vehicle ($n = 8$) or NPY (0.1 nmol, $n = 7$; 0.3 nmol, $n = 7$) on formalin-induced CPA. Data are expressed as means ± SEM. The columns show the time spent in the pain-paired compartment in the preconditioning (white columns) and test (black columns) sessions (*A*). $^{\#\#}p < 0.01$ compared with the preconditioning session (paired *t* test). The columns show CPA scores (*B*). $^{\#}p < 0.05$ compared with vehicle-injected rats (Newman–Keuls *post hoc* test). *C*, Effects of intra-dlBNST injection of vehicle ($n = 6$) or NPY (0.1 nmol, $n = 5$; 0.3 nmol, $n = 7$) on formalin-induced nociceptive behaviors. Data are expressed as means ± SEM.

Also, in the intra-dlBNST AS-30 (0.3 and 1 nmol/side)-injected groups, no significant difference ($t = 1.56$ (df = 5), $p > 0.05$ and $t = 1.51$ (df = 6), $p > 0.05$, respectively, paired *t* test) was observed in the time spent in the pain-paired compartment between the test (475 ± 20 and 502 ± 24 s, respectively) and the preconditioning (533 ± 32 and 535 ± 24 s, respectively) sessions. CPA scores showed dose-dependent attenuation of formalin-induced CPA by intra-dlBNST injection of these antagonists. As shown in Figure 3, *C* and *D*, one-way ANOVA indicated a significant

difference among groups (NBI27914, $F_{(2,19)} = 3.87$, $p < 0.05$ and AS-30, $F_{(2,16)} = 5.96$, $p < 0.05$). *Post hoc* comparisons revealed that NBI27914 at a dose of 1 nmol/side (37.6 ± 20.7 s; $p < 0.05$), but not 0.3 nmol/side (71.3 ± 32.5 s; $p > 0.05$), and AS-30 at doses of 0.3 and 1 nmol/side (58.3 ± 20.8 s, $p < 0.05$ and 33.3 ± 22.1 s, $p < 0.05$, respectively) attenuated formalin-induced CPA significantly compared with the vehicle-injected group (155 ± 34 s and 147 ± 30, respectively).

Because the dlBNST is located close to the lateral ventricle, it was possible that drugs leaking to the lateral ventricle might act on brain regions other than the dlBNST and suppress formalin-induced CPA. Thus, off-site control experiments were performed by injecting these antagonists into the lateral ventricle at a dose of 1 nmol/side. In the intracerebroventricularly injected NBI27914 and AS-30 groups ($n = 7$ each), the time spent in the pain-paired compartment during the test session (382 ± 23 and 452 ± 29 s, respectively) was significantly shorter ($t = 4.91$ (df = 6), $p < 0.01$ and $t = 3.61$ (df = 6), $p < 0.05$, respectively, paired t test) than the time during the preconditioning session (482 ± 8 and 535 ± 20 s, respectively). Thus, these results showed no suppressing effects of intracerebroventricularly administered NBI27914 and AS-30 on formalin-induced CPA, suggesting that the dlBNST was the likely site of action of these antagonists in suppressing formalin-induced CPA.

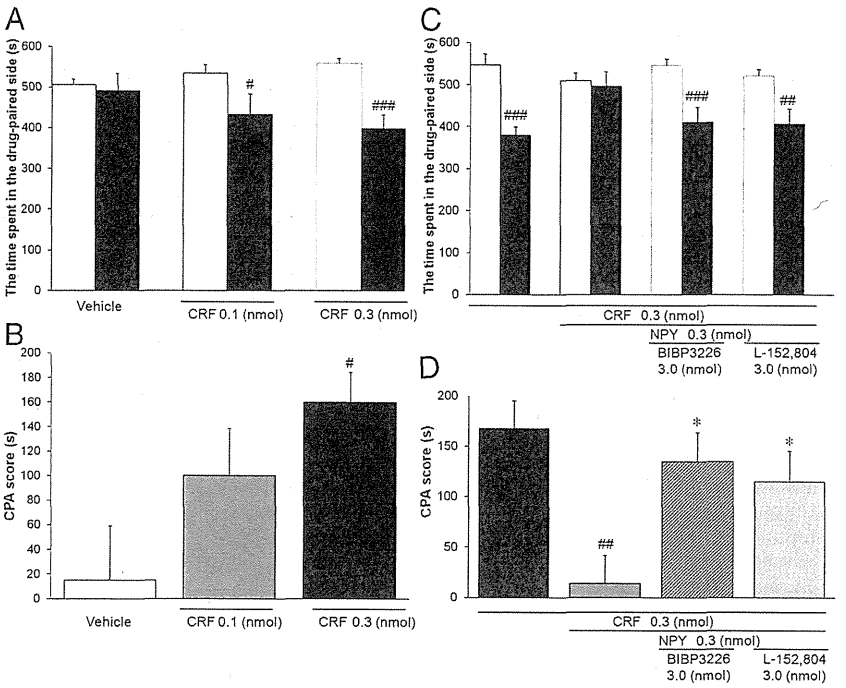

Figure 5. Effect of intra-dlBNST injection of NPY on CRF-induced CPA. ***A***, ***B***, Effects of intra-dlBNST injection of vehicle ($n = 10$) or CRF (0.1 nmol, $n = 10$; 0.3 nmol, $n = 11$) were examined using a place conditioning paradigm. Data are expressed as means ± SEM. ***A***, The columns show the time spent in the drug-paired compartment in the preconditioning (white columns) and test (black columns) sessions. $^{\#,\#\#\#}p < 0.05, 0.001$ compared with the preconditioning session (paired t test). ***B***, The columns show CPA scores. $^{\#}p < 0.05$ compared with vehicle-injected rats (Newman–Keuls *post hoc* test). ***C***, ***D***, Effects of intra-dlBNST injection of NPY in the presence or absence of subtype-selective NPY antagonists on CRF-induced CPA (CRF, $n = 10$; CRF + NPY, $n = 10$; CRF + NPY + BIBP3226, $n = 11$; CRF + N PY + L-152,804, $n = 12$). ***C***, The columns show the time spent in the drug-paired compartment in the preconditioning (white columns) and test (black columns) sessions. $^{\#\#,\#\#\#}p < 0.01, 0.001$ compared with the preconditioning session (paired t test). ***D***, The columns show CPA scores. $^{\#\#}p < 0.01$ compared with CRF alone-injected rats; $^{*}p < 0.05$ compared with CRF + NPY-injected rats (Newman–Keuls *post hoc* test).

To examine whether intra-dlBNST injection of NBI27914 or AS-30 per se produced conditioned place preference (CPP) or CPA, these drugs (1 nmol/side) were injected into the bilateral dlBNST in the absence of intraplantar formalin injection. In both the intra-dlBNST NBI27914- and AS-30-injected groups ($n = 6$ and $n = 7$, respectively), no significant difference ($t = 1.06$ (df = 5), $p > 0.05$ and $t = 0.12$ (df = 6), $p > 0.05$, respectively, paired t test) was observed in the time spent in the drug-paired compartment between the test (491 ± 22 and 487 ± 33 s, respectively) and preconditioning (509 ± 28 and 491 ± 10 s, respectively) sessions. CPA scores were 18.3 ± 17.3 and 4.14 ± 33.5 s, respectively, which were not significantly different ($t = 0.21$ (df = 9), $p > 0.05$ and $t = 0.51$ (df = 11), $p > 0.05$, respectively, Student's t test) from the CPA score of the vehicle-injected group (23.8 ± 19.2 s, $n = 5$ and 28.7 ± 34.8 s, $n = 6$, respectively). These data showed that neither CPP nor CPA was induced by the intra-dlBNST injection of these antagonists, indicating that these drugs have no motivational effect by themselves when injected into the dlBNST at these doses.

As shown in Figure 3*E*, intra-dlBNST injection of NBI27914 (0.3 nmol/side or 1 nmol/side) or AS-30 (0.3 nmol/side or 1 nmol/side) did not affect formalin-induced nociceptive behaviors compared with the vehicle-injected group. Two-way repeated-measures ANOVA revealed no significant effect of these drugs ($F_{(4,31)} = 1.05$; $p > 0.05$) and no significant interaction between the drugs and time ($F_{(44,341)} = 0.89$; $p > 0.05$). These results showed that intra-dlBNST injection of neither NBI27914 nor AS-30 affected the sensory component of pain.

Effects of intra-dlBNST injection of NPY on formalin-induced CPA and nociceptive behaviors

The effects of intra-dlBNST injection of NPY (0.1 and 0.3 nmol/side) on formalin-induced CPA were examined. In the intra-dlBNST vehicle-injected and NPY (0.1 nmol/side)-injected groups, the time spent in pain-paired compartment during the test session (408 ± 23 and 438 ± 33 s, respectively) was significantly shorter ($t = 3.81$ (df = 7), $p < 0.01$ and $t = 4.20$ (df = 6), $p < 0.01$, respectively, paired t test) than the time during the preconditioning session (553 ± 29 and 527 ± 22 s, respectively; Fig. 4*A*). In the intra-dlBNST NPY (0.3 nmol/side)-injected group, no significant difference ($t = 0.57$ (df = 6), $p > 0.05$, paired t test) was observed in the time spent in the pain-paired compartment between the test (504 ± 24 s) and preconditioning (520 ± 13 s) sessions. CPA scores showed dose-dependent attenuation of formalin-induced CPA by intra-dlBNST injection of NPY (Fig. 4*B*). One-way ANOVA indicated a significant difference among groups ($F_{(2,19)} = 4.51$, $p < 0.05$). *Post hoc* comparisons revealed that NPY at a dose of 0.3 nmol/side (15.7 ± 27.3 s, $p < 0.05$), but not 0.1 nmol/side (89.0 ± 21.2 s), attenuated formalin-induced CPA significantly compared with the vehicle-injected group (145 ± 38.0 s).

The effects of off-site control injections of NPY (0.3 nmol/side) into the lateral ventricle on formalin-induced CPA were examined. In the intracerebroventricular NPY-injected group ($n = 7$), the time

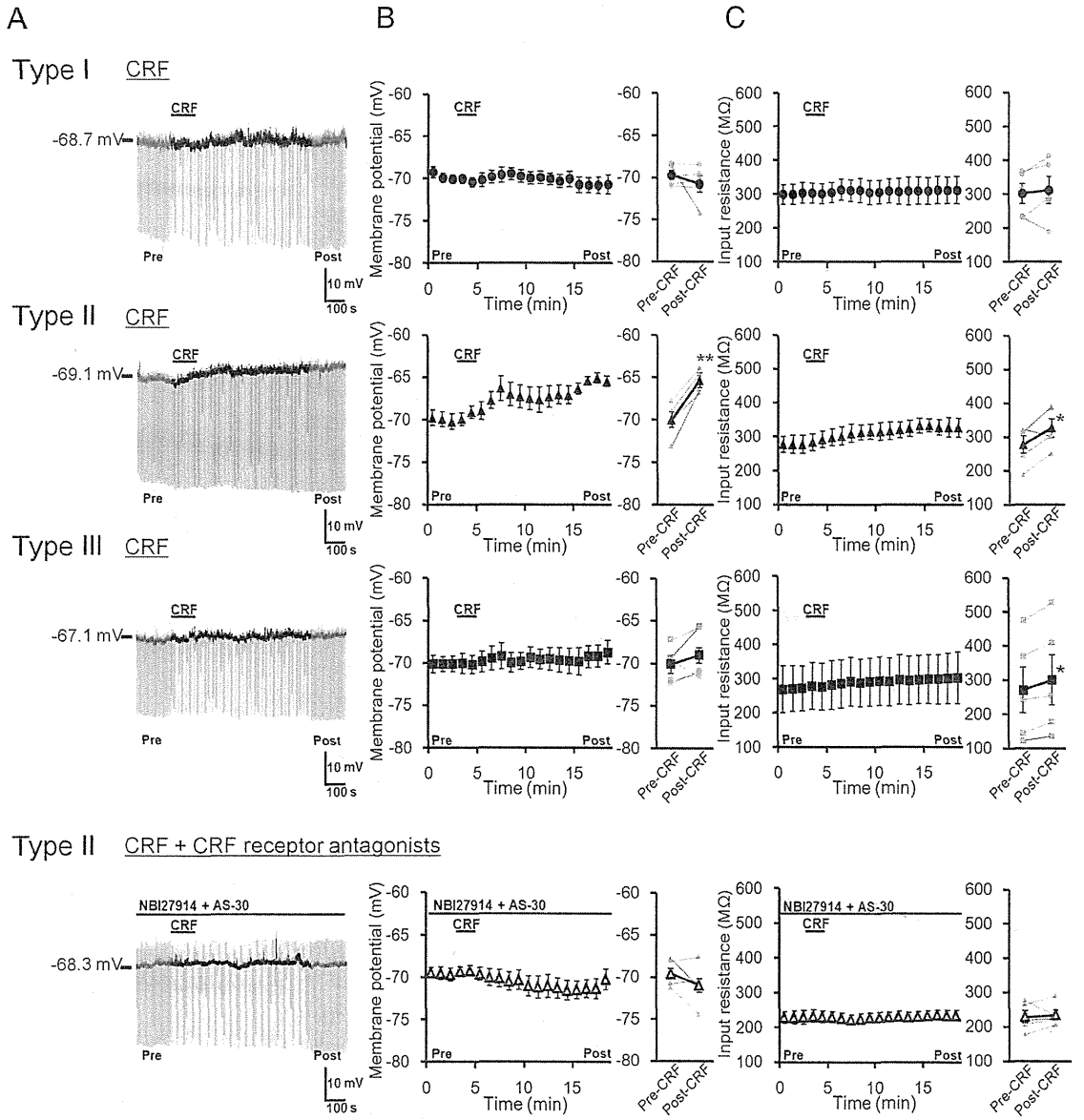

Figure 6. Effects of CRF on membrane potential and input resistance in three types of dlBNST neurons. ***A***, Representative traces from current-clamp recordings in type I (top), type II (second row), and type III (third row) dlBNST neurons, and type II dlBNST neurons in the presence of NBI27914 (300 nM) + AS-30 (300 nM) (bottom). ***B***, ***C***, Effects of CRF (1 μM, 2 min) on membrane potential (***B***) and input resistance (***C***) in type I ($n = 5$; top), type II ($n = 5$; second row), and type III ($n = 5$; third row) dlBNST neurons, and type II dlBNST neurons in the presence of NBI27914 + AS-30 ($n = 5$; bottom). Left, Time courses of membrane potential (***B***) and input resistance (***C***). Right, Averaged membrane potential (***B***) and input resistance (***C***) in the period of pre-CRF (0–3 min) and post-CRF (16–19 min) application. Gray symbols and lines show data obtained from individual neurons, and black symbols and lines show averaged data obtained from five neurons. Data are expressed as means ± SEM. $^{*}p < 0.05$, $^{**}p < 0.01$ compared with pre-CRF application (paired *t* test).

spent in the pain-paired compartment during the test session was 448 ± 30 s, which was significantly shorter ($t = 3.13$ (df = 6), $p < 0.05$, paired *t* test) than the time during the preconditioning session (553 ± 25 s). This result showed no suppressing effect of intracerebroventricularly administered NPY on formalin-induced CPA, suggesting that the dlBNST was the likely site of action of this peptide in suppressing formalin-induced CPA.

To examine whether intra-dlBNST injection of NPY per se produced CPP or CPA, NPY (0.3 nmol/side) was injected into the bilateral dlBNST in the absence of intraplantar formalin injection. In the intra-dlBNST NPY-injected group ($n = 5$), no significant difference ($t = 0.42$ (df = 4), $p > 0.05$, paired *t* test) was observed in the time spent in the drug-paired compartment between the test (501 ± 40 s) and preconditioning (488 ± 10 s) sessions. The CPA score (–13.4 ± 32.3 s) was not significantly different ($t = 0.09$ (df = 7), $p > 0.05$, Student's *t* test) from that of the vehicle-injected group (–18.3 ± 41.5 s, $n = 4$). These findings showed that neither CPP nor CPA was induced by the intra-dlBNST injection of NPY, indicating that this peptide has no motivational effect by itself when injected into the dlBNST at this dose.

As shown in Figure 4*C*, intra-dlBNST injection of NPY (0.1 nmol/side or 0.3 nmol/side) did not affect formalin-induced nociceptive behaviors compared with the vehicle-injected group. Two-way repeated-measures ANOVA revealed no significant effect of intra-dlBNST NPY ($F_{(2,15)} = 0.22$; $p > 0.05$) and no significant interaction between the drugs and time ($F_{(22,165)} = 0.48$; $p > 0.05$). These results showed that intra-dlBNST injection of NPY did not affect the sensory component of pain.

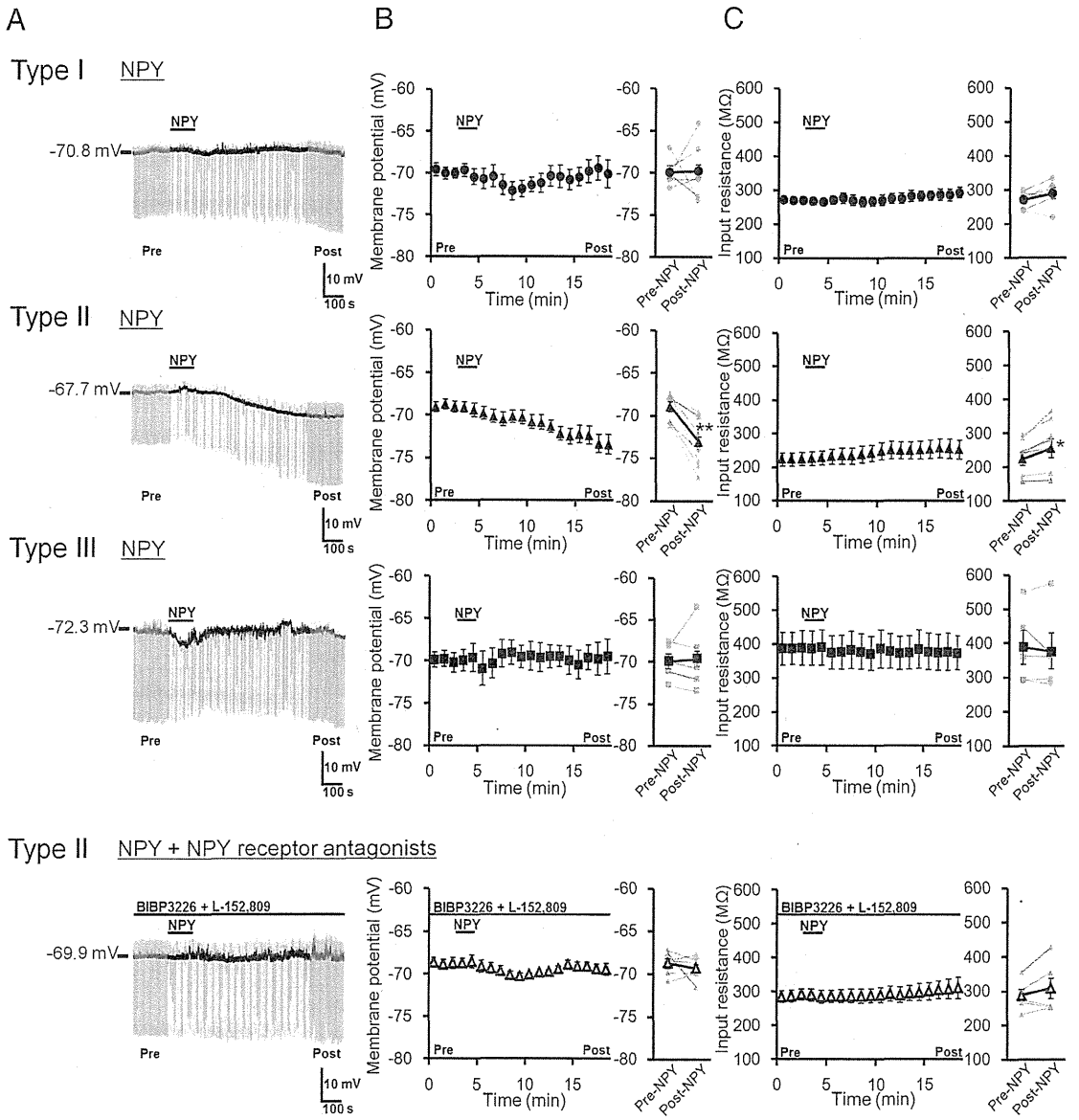

Figure 7. Effects of NPY on membrane potential and input resistance in three types of dlBNST neurons. ***A***, Representative traces from current-clamp recordings in type I (top), type II (second row), and type III (third row) dlBNST neurons, and type II dlBNST neurons in the presence of BIBP3226 (1 μM) + L-152,804 (1 μM) (bottom). ***B***, ***C***, Effects of NPY (1 μM, 2 min) on membrane potential (***B***) and input resistance (***C***) in type I ($n = 6$; top), type II ($n = 8$; second row), and type III ($n = 5$; third row) dlBNST neurons, and type II dlBNST neurons in the presence of BIBP3226 + L-152,804 ($n = 6$; bottom). Left, Time courses of membrane potential (***B***) and input resistance (***C***). Right, Averaged membrane potential (***B***) and input resistance (***C***) in the period of pre-NPY (0–3 min) and post-NPY (16–19 min) application. Gray symbols and lines show data obtained from individual neurons, and black symbols and lines show averaged data obtained from 5–8 neurons. Data are expressed as means ± SEM. $^{*}p < 0.05$, $^{**}p < 0.01$ compared with pre-NPY application (paired *t* test).

Effect of intra-dlBNST injection of NPY on CRF-induced CPA

Sahuque et al. (2006) reported that intra-BNST administration of CRF produced a dose-dependent CPA. First, we confirmed the induction of CPA by the intra-dlBNST injection of CRF. As shown in Figure 5*A*, in rats injected with CRF at doses of 0.1 and 0.3 nmol/side, the time spent in the drug-paired compartment during the test session (434 ± 49 and 399 ± 34 s, respectively) was significantly shorter ($t = 2.64$ (df = 9), $p < 0.05$ and $t = 6.50$ (df = 10), $p < 0.001$, respectively, paired *t* test) than the time during the preconditioning session (534 ± 21 and 558 ± 13 s, respectively). CPA scores revealed a dose-dependent induction of CPA by intra-dlBNST injection of CRF (Fig. 5*B*). One-way ANOVA indicated a significant difference among groups ($F_{(2,28)} = 4.15$, $p < 0.05$). *Post hoc* comparisons showed that CRF at a dose of 0.3 nmol/side (160 ± 25 s, $p < 0.05$), but not 0.1 nmol/side (99.4 ± 38.2 s, $p > 0.05$), significantly induced CPA compared with the vehicle-treated group (15.1 ± 44.1 s).

Next, the effect of coadministration of NPY on CRF-induced CPA was examined. In the rats simultaneously injected with CRF (0.3 nmol/side) and NPY (0.3 nmol/side), no significant difference ($t = 0.40$ (df = 9), $p > 0.05$, paired *t* test) was observed in the time spent in the drug-paired compartment between the test (496 ± 34 s) and preconditioning (510 ± 18 s) sessions (Fig. 5*C*). Coadministration of NPY with CRF significantly ($t = 3.43$ (df = 18), $p < 0.01$, Student's *t* test) reduced the CPA score (14.0 ± 35.3 s) compared with the CRF alone-injected group (167.7 ± 87.2 s; Fig. 5*D*).

To examine whether intra-dlBNST repeated injections of NPY per se produced CPP or CPA, NPY (0.3 nmol/side; $n = 6$)

was administered into the bilateral dlBNST in the absence of CRF over 3 d. No significant difference ($t = 0.48$ (df = 5), $p > 0.05$, paired t test) was observed in the time spent in the drug-paired compartment between the test (524 ± 19 s) and preconditioning (516 ± 21 s) sessions. The CPA score (−8.00 ± 16.8 s) was not significantly different ($t = 0.39$ (df = 14), $p > 0.05$, Student's t test) from that of the vehicle-injected group (15.1 ± 44.1 s, $n = 10$). These data showed that neither CPP nor CPA was induced by intra-dlBNST repeated injections of NPY alone, indicating that NPY had no motivational effect by itself when repeatedly injected into the dlBNST at this dose.

To identify the receptor subtype(s) involved in the inhibitory effect of NPY on CRF-induced CPA, the effects of coadministration of BIBP3226 (Y_1 selective antagonist) or L-152,804 (Y_5 selective antagonist) were examined. In the groups coadministered BIBP3226 (3.0 nmol/side) or L-152,804 (3.0 nmol/side) in addition to CRF and NPY, significant differences ($t = 4.68$ (df = 10), $p < 0.001$ or $t = 3.71$ (df = 11), $p < 0.01$, respectively, paired t test) were observed in the time spent in the drug-paired compartment between the test (412 ± 35 or 407 ± 35 s, respectively) and preconditioning (546 ± 16 or 521 ± 16 s, respectively) sessions (Fig. 5*C*). CPA scores of these groups (134 ± 29 or 114 ± 31 s, respectively) increased significantly ($t = 2.67$ (df = 19), $p < 0.05$ or $t = 2.15$ (df = 20), $p < 0.05$, respectively, Student's t test) compared with the score of the group injected with CRF and NPY (14.0 ± 35.3 s) (Fig. 5*D*).

Effects of CRF and NPY on membrane potentials in dlBNST neurons

Effects of CRF and NPY on the membrane potentials in dlBNST neurons were examined using a whole-cell patch-clamp technique in slice preparations. First, we examined the effects of a 2 min bath application of 1 μM CRF on membrane potentials in dlBNST neurons (Fig. 6). In type I neurons, CRF did not affect the membrane potential (−69.74 ± 0.55 and −70.76 ± 0.99 mV in the periods before and after CRF application, respectively; $t = 0.86$ (df = 4), $p > 0.05$, paired t test; Fig. 6*B*, top), and the input resistance was not changed (301.0 ± 29.5 and 311.4 ± 40.2 MΩ in the periods before and after CRF application, respectively; $t = 0.50$ (df = 4), $p > 0.05$, paired t test; Fig. 6*C*, top). On the other hand, CRF depolarized membrane potentials gradually in all of the type II neurons tested ($n = 5$). CRF application significantly changed the membrane potential from −69.97 ± 0.90 mV to −65.33 ± 0.56 mV ($t = 7.59$ (df = 4), $p < 0.01$, paired t test; Fig. 6*B*, second row). The input resistance in the postdrug period (327.0 ± 26.8 MΩ) was significantly higher than that in the predrug period (277.4 ± 26.0 MΩ; $t = 2.79$ (df = 4), $p < 0.05$, paired t test; Fig. 6*C*, second row). The CRF-induced depolarization and increase in input resistance were not observed in the presence of CRF receptor antagonists (300 nM NBI27914 + 300 nM AS-30), indicating that these changes were mediated by activation of CRF receptors (−69.59 ± 0.71 and −70.99 ± 1.10 mV before and after CRF application, respectively; $t = 1.66$ (df = 4), $p > 0.05$, paired t test; Fig. 6*B*, bottom; 228.9 ± 18.5 and 234.5 ± 14.3 MΩ before and after CRF application, respectively; $t = 0.41$ (df = 4), $p > 0.05$, paired t test; Figure 6*C*, bottom). Although CRF increased the input resistance in type III neurons slightly, but significantly (270.6 ± 67.0 and 300.5 ± 73.6 MΩ in the periods before and after CRF application, respectively; $t = 3.71$ (df = 4), $p < 0.05$, paired t test; Fig. 6*C*, third row), the membrane potential was not affected by CRF (−70.14 ± 0.95 and −69.05 ± 1.35 mV in the periods before and after CRF application, respectively; $t = 1.20$ (df = 4), $p > 0.05$, paired t test; Fig. 6*A*,*B*, third row) in this type of neurons.

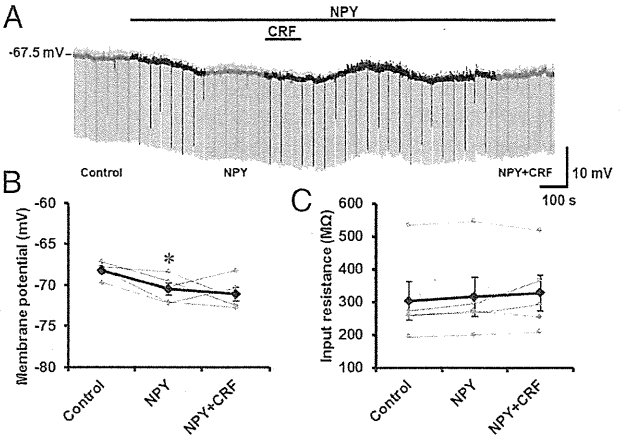

Figure 8. Inhibitory effects of NPY on CRF-induced depolarization in type II dlBNST neurons. ***A***, Representative trace from current-clamp recording in a type II dlBNST neuron. The effects of the peptides were evaluated in the periods indicated by shading (Control, 0–3 min before NPY application; NPY, 0–3 min before CRF application; NPY + CRF, 12–15 min after CRF application). ***B***, ***C***, Effects of CRF on membrane potential (***B***) and input resistance (***C***) in the presence of NPY. Gray symbols and lines show data obtained from individual neurons ($n = 5$), and black symbols and lines show averaged data obtained from five neurons. *$p < 0.05$ compared with control (Newman–Keuls *post hoc* test).

Next, we investigated the effects of a 2 min bath application of 1 μM NPY on the membrane potentials in dlBNST neurons (Fig. 7). In type I neurons, NPY did not affect either the membrane potential (−69.89 ± 0.66 and −69.78 ± 1.44 mV in the periods before and after NPY application, respectively; $t = 0.06$ (df = 5), $p > 0.05$, paired t test; Fig. 7*A*,*B*, top), and the input resistance (270.2 ± 10.1 and 288.5 ± 16.4 MΩ in the periods before and after NPY application, respectively; $t = 1.82$ (df = 5), $p > 0.05$, paired t test; Fig. 7*C*, top). On the other hand, NPY hyperpolarized membrane potentials gradually in all of the type II neurons tested ($n = 8$). NPY application significantly changed membrane potential from −68.91 ± 0.59 to −73.05 ± 1.06 mV ($t = 5.39$ (df = 7), $p < 0.01$, paired t test; Fig. 7*B*, second row). The input resistance in the postdrug period (254.9 ± 28.5 MΩ) was significantly larger than that in the predrug period (223.7 ± 19.5 MΩ; $t = 3.15$ (df = 7), $p < 0.05$, paired t test; Fig. 7*C*; second row). In the presence of NPY receptor antagonists (1 μM BIBP3226 + 1 μM L-152,804), NPY did not affect either the membrane potentials (−68.75 ± 0.56 and −69.35 ± 0.56 mV before and after NPY application, respectively; $t = 0.82$ (df = 5), $p > 0.05$, paired t test; Fig. 7*B*, bottom) or the input resistance (287.5 ± 16.9 and 307.9 ± 28.9 MΩ before and after NPY application, respectively; $t = 1.41$ (df = 5), $p > 0.05$, paired t test; Fig. 7*C*, bottom), suggesting that the effects of NPY were mediated via NPY receptors. In type III neurons, NPY did not affect either the membrane potential (−69.94 ± 0.96 and −69.61 ± 1.77 mV in the periods before and after NPY application, respectively; $t = 0.29$ (df = 4), $p > 0.05$, paired t test; Fig. 7*B*, third row) or the input resistance (387.8 ± 49.2 and 376.2 ± 52.5 MΩ in the periods before and after NPY application, respectively; $t = 0.68$ (df = 4), $p > 0.05$, paired t test; Fig. 7*C*, third row).

The opposing effects of CRF and NPY on the membrane potential in type II dlBNST neurons allowed us to examine the effects of NPY on CRF-induced depolarization (Fig. 8). As seen in Figure 8, *A* and *B*, in type II neurons, significant hyperpolarization was observed after NPY application (−68.20 ± 0.43 and −70.46 ± 0.75 mV in the periods before and after NPY application, respectively; $p < 0.05$, compared with the pre-application of drugs (Control), one-way repeated measured ANOVA ($F_{(2,8)} =$

4.83, $p < 0.05$) with Bonferroni's *post hoc* test, $n = 5$;Figure 8*B*). In the presence of NPY, CRF did not depolarize the membrane potential in type II neurons (–70.46 ± 0.75 and –71.06 ± 0.83 mV in the periods before and after CRF application, respectively; Fig. 8*B*). We occasionally observed a transient excitation after CRF application in the presence of NPY (Fig. 8*A*). However, the depolarization was very small and did not persist over ~16 min, where CRF usually exhibits maximal depolarization in the absence of NPY. The input resistance was also unaltered by CRF in the presence of NPY (316.1 ± 59.8 and 328.0 ± 54.3 MΩ in the periods before and after CRF application, respectively; Fig. 8*C*).

Conductances associated with the actions of CRF and NPY in type II dlBNST neurons

To investigate the conductances underlying the actions of CRF and NPY, we studied the effects of these peptides on the steady-state *I–V* relationships in type II neurons by applying a voltage ramp protocol. As shown in Figure 9, *A* and *B*, CRF-induced net currents in individual neurons were heterogeneous: CRF decreased net currents in some neurons ($n = 4$, Fig. 9*A*, left, *B*, black traces), while the increase in net currents was observed in other neurons ($n = 6$; Fig. 9*A*, right, *B*, gray traces). Thus, we classified these neurons into two groups and designated them as type IIa and type IIb. The averaged current trace of type IIa neurons revealed that the reversal potential of this current was approximately –95 mV (–94.4 ± 3.9 mV, $n = 4$), which is close to the potassium equilibrium potential (–109.3 mV) calculated from the Nernst equation under our experimental conditions (Fig. 9*C*, left). On the other hand, the CRF-induced increased currents reversed the polarity at approximately –50 mV (–55.9 ± 6.1 mV, $n = 6$) with a clear outward rectification in type IIb neurons, suggesting a contribution of nonselective cationic conductance (Takano et al., 1996; Yang and Ferguson, 2002; Murai and Akaike, 2005; Kaneko et al., 2008) (Fig. 9*C*, right). CRF significantly increased negative holding currents (–58.92 ± 8.54 and –67.77 ± 9.63 pA before and after CRF application, respectively; $t = 2.80$ (df = 9), $p < 0.05$, paired *t* test; Fig. 9*D*, upper), whereas the input resistance was not affected by CRF (339.9 ± 36.3 and 342.5 ± 39.1 MΩ before and after CRF application, respectively; $t = 0.31$ (df = 9), $p > 0.05$, paired *t* test; Fig. 9*D*, lower). These results suggest that at least two conductances might be associated with the CRF-induced depolarization. We observed the different effects of CRF on changes in input resistance between voltage- and current-clamp recordings. Voltage-clamp recordings were obtained from four type IIa and six type IIb neurons, which exhibited increased and decreased input resistance after CRF application, respectively. Thus, the apparent net change in input resistance seemed to be unchanged. On the other hand, in current-clamp recordings (Fig. 6), averaged input resistance was increased following CRF application. Although we did not determine the cell classes (IIa or IIb) in the current-clamp recording experiment, based on the changes in input resistance observed in individual neurons, it might be possible that the recorded neurons included four type IIa and one type IIb neurons.

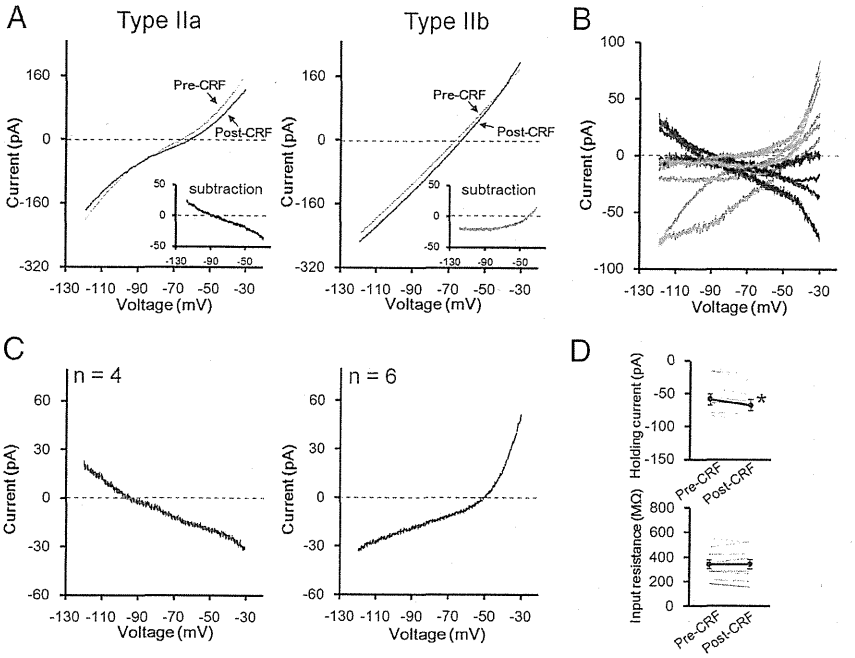

Figure 9. Conductances associated with the action of CRF in the type II dlBNST neurons. ***A***, Representative steady-state current responses to voltage ramp pulses from –30 to –120 mV recorded from type IIa (left) and type IIb (right) neurons in the periods of pre-CRF (gray) and post-CRF (black) application (1 μM, 2 min). The insets show the subtraction of the currents (CRF-induced net currents). Axis titles in ***A*** apply in the insets. ***B***, Traces of CRF-induced net currents in four type IIa (black) and six type IIb (gray) neurons. ***C***, Average traces of CRF-induced currents in type IIa ($n = 4$, left) and type IIb ($n = 6$, right) neurons. Gray shadows represent SEM. Vertical dashed lines show the reversal potential. ***D***, Effects of CRF on the holding currents at –70 mV (upper) and the input resistance (lower). Gray lines represent the data obtained from individual neurons ($n = 10$), and black symbols and lines show the averaged data obtained from 10 neurons. *$p < 0.05$ compared with pre-CRF application (paired *t* test).

On the other hand, NPY-induced net currents in individual neurons were similar in all of the neurons tested: NPY decreased net currents in all recorded neurons ($n = 8$, Fig. 10*A*,*B*). This result suggests that type II neurons cannot be classified according to the response to NPY. In other words, both type IIa and IIb neurons may respond to NPY in the same manner. NPY-induced change in the net currents was accompanied by significantly reduced negative holding currents (–62.64 ± 10.06 and –54.81 ± 10.12 pA before and after NPY application, respectively; $t = 4.05$ (df = 7), $p < 0.01$, paired *t* test; Fig. 10*C*, upper) and increased input resistance (304.3 ± 30.3 and 359.9 ± 48.6 MΩ before and after NPY application, respectively; $t = 2.37$ (df = 7), $p < 0.05$, paired *t* test; Fig. 10*C*, lower). The averaged trace exhibited that the current associated with NPY reversed the polarity approximately –60 mV (–60.4 ± 6.0 mV, $n = 8$; Fig. 10*B*), suggesting a contribution of multiple conductances to the action of NPY. One of the candidate conductances is hyperpolarization-activated current (I_h), the suppression of which has been shown to be critical for NPY-induced hyperpolarization in the BLA (Giesbrecht et al., 2010). Thus, we tested this hypothesis by using I_h blocker ZD7288 (Fig. 10*D–F*). Bath application of 10 μM ZD7288 alone elicited significant hyperpolarizing currents (–31.72 ± 8.62 and –11.43 ± 6.70 pA in the periods 0–3 min before and 7–10 min after ZD7288 application, respectively; $t = 3.66$ (df = 7), $p < 0.01$, paired *t* test, $n = 8$) and increased input resistance (482.21 ± 36.7 and 744.9 ± 124.6 MΩ in the periods 0–3 min before and 7–10 min after ZD7288 application, respectively; *t* =